

Criteria for sprites and elves based on Schumann resonance observations

E. Huang,¹ E. Williams,² R. Boldi,³ S. Heckman,⁴ W. Lyons,⁵ M. Taylor,⁶ T. Nelson,⁵ and C. Wong⁷

Abstract. Ground flashes with positive polarity associated with both sprites and elves excite the Earth's Schumann resonances to amplitudes several times greater than the background resonances. Theoretical predictions for dielectric breakdown in the mesosphere are tested using ELF methods to evaluate vertical charge moments of positive ground flashes. Comparisons of the measured time constants for lightning charge transfer with the electrostatic relaxation time at altitudes of nighttime sprite initiation (50–70 km) generally validate the electrostatic assumption in predictions made initially by *Wilson* [1925]. The measured charge moments ($Q dS = 200\text{--}2000$ C-km) are large in comparison with ordinary negative lightning but are generally insufficient to account for conventional air breakdown at sprite altitudes. The measured charge moments, however, are sufficient to account for electron runaway breakdown, and the long avalanche length in this mechanism also accounts for the exclusive association of sprites with ground flashes of positive polarity. The association of elves with large peak currents (50–200 kA) measured by the National Lightning Detection Network in a band pass beyond the Schumann resonance range is consistent with an electromagnetic pulse mechanism for these events.

1. Introduction

Sprites and elves are newly discovered optical phenomena in the mesosphere over large thunderstorms [*Franz et al.*, 1990; *Lyons*, 1994; *Sentman et al.*, 1995]. Previous studies have also established a link between individual positive ground flashes that stimulate sprites (Figure 1) and the global excitation of Schumann resonances within the Earth-ionosphere cavity [*Boccippio et al.*, 1995]. The present study concerns the use of quantitative Schumann resonance methods from a single station [*Burke and Jones*, 1995] to characterize the lightning source (e.g., location, current, and charge moment) and thereby establish criteria for sprite occurrences. The traditional method for measuring the charge moment of a lightning flash is electrostatic and is distinguished from the electromagnetic method used in this study.

Initial efforts to establish empirical rules for sprite and elve occurrence on the basis of observations from the National Lightning Detection Network (NLDN) have met with limited success. Sprites and elves occur almost exclusively with positive ground flashes, but the majority of positive ground flashes are not linked with sprites. Larger-than-average NLDN peak currents (>30 kA) are associated with sprite events [*Boccippio et al.*, 1995; *Lyons*, 1996b], but very large peak currents (>90 kA) are often linked with elves rather than sprites. The “slow-tail” ELF signature has been linked with sprites [*Reising et al.*, 1996] and is often incorrectly interpreted as a unique manifestation of a continuing current [*Wait*, 1960], which is common without an accompanying sprite. One assumption made early on was that a large-amplitude NLDN event (in terms of peak current) is more likely to create a sprite or an elve and that sprite size should increase with higher peak current. Results here show that amplitude is not a good indicator of sprite occurrence. The present study shows that total charge transfer is a better indicator and that little correlation exists between the NLDN peak current and the total charge transfer for positive ground flashes. Clearly, new methods are needed to quantitatively predict lightning-induced optical phenomena in the mesosphere.

As it turns out, *Wilson* [1916, 1925, 1956] speculated more than 70 years ago about discharges in the upper atmosphere and suggested simple electrostatic criteria for their appearance. More recently, elaborate theoretical models have been developed for sprites and elves on the basis of a tropospheric lightning source [*Pasko et al.*, 1995; *Bell et al.*, 1995; *Inan et al.*, 1996b]. In this paper we return to the simpler ideas of *Wilson* to evaluate lightning source charac-

¹Department of Electrical Engineering and Computer Science, Massachusetts Institute of Technology, Cambridge.

²Parsons Laboratory, Massachusetts Institute of Technology, Cambridge.

³Lincoln Laboratory, Massachusetts Institute of Technology, Lexington.

⁴NASA Marshall Space Flight Center, Huntsville, Alabama.

⁵FMA Research, Inc., Fort Collins, Colorado.

⁶Space Dynamics Laboratory, Utah State University, Logan.

⁷J. P. Morgan Securities Asia Pte. Ltd., Singapore.

Copyright 1999 by the American Geophysical Union.

Paper number 1999JD900139.
0148-0227/99/1999JD900139\$09.00

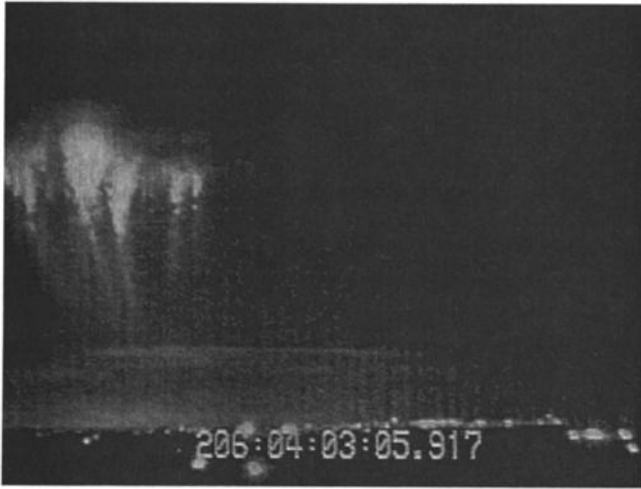


Figure 1. A sample sprite photo documented from the Yucca Ridge Field Station.

teristics quantitatively from calibrated Schumann resonance observations.

2. Theoretical Considerations

2.1. Dielectric Breakdown in the Upper Atmosphere

In the early part of this century, C.T.R. Wilson laid down the fundamental ideas on the thunderstorm-induced electrical perturbation of the upper atmosphere. In 1916, Wilson had considered the possible influence of the conductive upper atmosphere on his electrostatic measurement of the charge structure of thunderclouds. His conclusion, "It is unlikely that the requisite high conductivity could under normal conditions extend sufficiently low in the atmosphere to be an important factor in the problem," was followed by speculation about the electric field of lightning causing ionization of the mesosphere [Wilson, 1916, p. 573]:

There is, however, the possibility that the electric force produced by a lightning discharge below it might exceed that required to cause ionization by collisions. A lightning flash might thus be accompanied by a high level discharge extending as a sheet (possibly visible as sheet lightning) throughout the whole region in which the electric force and the pressure lay within the proper limits.

A more quantitative statement of the same idea for a static thundercloud appeared in a later work by Wilson [1925, p. 33D]:

The electric force due to a cloud of moment M , at a point vertically above it in the atmosphere may be taken as approximately $2M/4\pi\epsilon_0 r^3$, where r is the height of the point above ground. While the electric force due to a thundercloud falls off rapidly as r increases, the electric force required to cause sparking (which for a given composition of the air is proportional to density)

falls off still more rapidly. Thus if the electric moment of a cloud is not too small, there will be a height above which the electric force due to the cloud exceeds the sparking limit.

In the same paper, Wilson [1925, p. 33D] went on to discuss conditions at 60 km altitude, which is the typical initiation height for sprites found in recent observations [Fukunishi et al., 1996]. Wilson continues:

At a height of 60 km, the density of the air is about 1.6×10^{-4} of that near the ground, while the composition of the air is not very different, so that the critical value of the field may be taken as $30,000 \times 1.6 \times 10^{-4} = 480$ volt/meter. To produce such a field at this height a thundercloud would require to have an electric moment of 1.7×10^{18} esu cm (5000 C-km). If we assume the critical field to remain proportional to the pressure, a thundercloud with an electric moment of about 1/10 of the above value (i.e., only a few times the electric moment of an ordinary lightning flash) would produce a field exceeding the critical value at a height of 80 km. Thus if there were no already existing conducting layer there is little doubt that a thundercloud would itself cause ionization in the upper atmosphere.

These statements pertain to the static charge moment of a thundercloud, but 40 years later, Wilson [1956, p. 315] applied this to the earlier speculation that the moment change due to lightning was necessary for a discharge to the upper atmosphere: "It is quite possible that a discharge between the top of the cloud and the ionosphere is a normal accompaniment of a lightning discharge to Earth."

These various ideas are illustrated quantitatively in Figure 2, referred to as the C.T.R. Wilson diagram. This plot

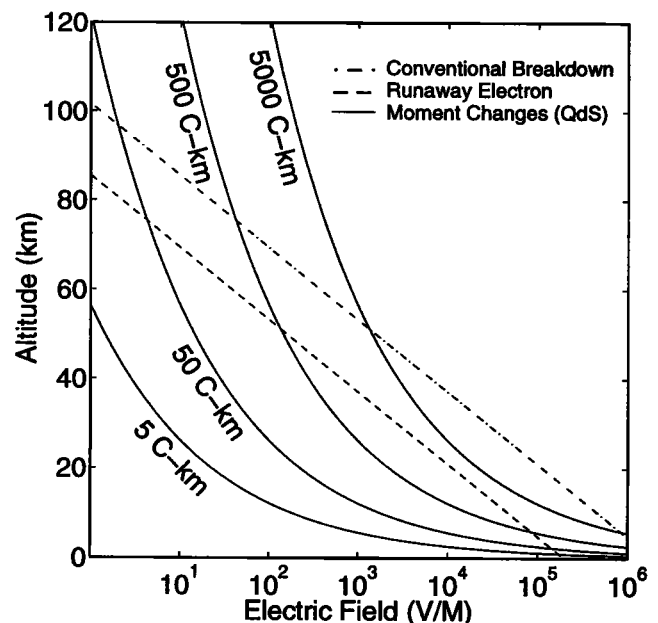


Figure 2. Breakdown electric field versus height and charge moment.

of the logarithm of the electric field versus altitude includes the decline of electric field with altitude associated with a vertical dipole moment ($M = Q dS$) at the Earth's surface:

$$\Delta E = \frac{1}{4\pi\epsilon_0} \frac{2M}{r^3} \left[\frac{V}{m} \right]. \quad (1)$$

Electric field variations associated with moments range in value from small intracloud discharges (~ 10 C-km) and ordinary negative ground flashes (~ 100 C-km [Krider, 1989]), to values documented later in Section 4.2 for positive ground flashes which cause sprites (~ 1000 C-km). Also shown in Figure 2 is the behavior of dielectric strength versus altitude. Since the dielectric strength of any gas is fundamentally proportional to density (rather than pressure) and since density declines approximately exponentially with altitude (with a scale height close to 7 km [Whipple, 1954]), the variation of dielectric strength is nearly a straight line in Figure 2. Two curves for breakdown strength are shown: (1) the one pertaining to the conventional air breakdown that Wilson envisioned and (2) the theoretical prediction for electron runaway breakdown from Gurevich *et al.* [1992]. The latter curve is given by

$$E(z) = 218 \frac{\rho(z)}{\rho(0)} \left[\frac{kV}{m} \right], \quad (2)$$

where $\rho(z)$ is the altitude dependent density of air.

Consistent with Wilson's [1925] previous statement, for every value of moment change exists a critical altitude at which the local electric field exceeds the local dielectric strength. The precise location of breakdown is not predicted, but the altitude range over which breakdown could initiate is bounded by the respective breakdown lines. Uncertainty in the altitude of sprite initiation causes uncertainty in the moment change required for breakdown.

2.2. Relaxation Time in the Mesosphere

The predictions of Figure 2 are strictly valid if the upper atmosphere is non-conductive, as Wilson [1916] himself noted. In response to the field increase of a lightning ground flash, the conductive upper atmosphere nullifies the imposed electric field. The local response time is the electrostatic relaxation time (ϵ/σ) whose altitude dependence was considered by Hale [1984] and by Roussel-Dupr e and Gurevich [1996]. This dependence is plotted in Figure 3 for both daytime and nighttime ionospheric conditions at midlatitude [Hale, 1984]. If the moment change occurs in a time short in comparison with the local relaxation time, the predictions in Figure 2 should be accurate. The timescale for charge transfer is therefore of major importance in the ELF observations to be discussed.

2.3. Excitation of the Earth-Ionosphere Cavity

On the basis of the simultaneous sprite and electromagnetic observations of Boccippio *et al.* [1995], the assumption is that the positive ground flash associated with the sprites and elves also excites ELF radiation in the Earth-ionosphere cavity. From the models of Wait [1996], Jones [1967], and Ishaq and Jones [1977], the frequency-dependent normal

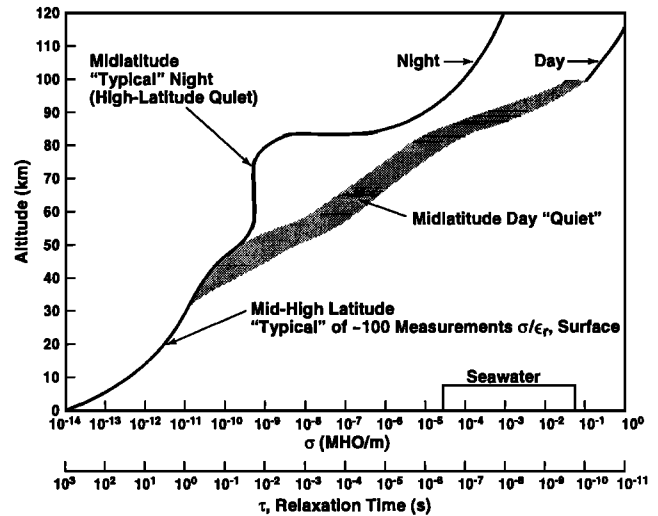


Figure 3. Electrostatic relaxation time versus altitude (adapted from Hale [1984]).

mode equations for the electric and magnetic fields are obtained:

$$E_z(f) = i \frac{I(f) dS \nu(\nu+1) P_\nu^0(-\cos\theta)}{4a^2 \epsilon_0 2\pi f h \sin(\pi\nu)} \left[\frac{V}{m \cdot Hz} \right], \quad (3)$$

$$H_\phi(f) = - \frac{I(f) dS P_\nu^1(-\cos\theta)}{4ah \sin(\pi\nu)} \left[\frac{A}{m \cdot Hz} \right], \quad (4)$$

respectively. These fields are produced by a cloud-to-ground (CG) lightning stroke in an idealized, spherically symmetric Earth-ionosphere cavity. In (3) and (4), $P_\nu^0(x)$ and $P_\nu^1(x)$ are Legendre functions with complex subscripts, $I(f) dS$ is the vertical current moment of the lightning ground flash, and ν is the complex eigenvalue which describes the propagation and dissipation characteristics of the atmosphere as a function of frequency. The variables a and h are the radius of the Earth (6.37 Mm) and the height of the ionosphere (80 km), respectively, θ is the great circle distance between the lightning and receiver, ϵ_0 is the permittivity, and i is the square root of -1 .

The complex eigenvalue ν can be calculated by the following equations:

$$\nu(f) [\nu(f) + 1] = (kaS)^2, \quad (5)$$

$$S = \left(\frac{C}{V} \right) - i \left(5.49 \frac{\alpha}{f} \right), \quad (6)$$

$$\frac{C}{V} = 1.64 - 0.1759 \ln f + 0.01791 (\ln f)^2, \quad (7)$$

$$\alpha = 0.063 f^{0.64} \left[\frac{dB}{Mm} \right], \quad (8)$$

where k is the wavenumber, S is the sine of the mode eigenangle, C is the speed of light, V is the phase velocity, α is the attenuation constant, and $f = \omega/2\pi$ is the frequency [Jones, 1967]. The quantities C/V and α are both values derived from Ishaq and Jones's [1977] numerical model for the ionosphere that used a measured ionospheric profile [Jones, 1967].

2.4. Wave Impedance

The current moments of the parent positive ground flashes are major targets in this study, but they cannot be determined from (3) and (4). Comparisons must be made with the wave impedance (E/H), which depends only on the source-receiver distance and not on the form of the source current [Jones and Kemp, 1971]. The formula for the wave impedance is

$$Z(f) = -i \frac{\nu(\nu+1) P_\nu^0(-\cos\theta)}{a\epsilon_0 2\pi f P_\nu^1(-\cos\theta)} [\Omega]. \quad (9)$$

The wave impedance is a unique function of the source-receiver separation and can be used to determine the distance to the lightning source [Jones and Kemp, 1971]. By comparing the recorded wave impedance with the theoretical waveforms, the range to the source can be estimated with an error on the order of several hundred kilometers [Burke and Jones, 1995; Boccippio et al., 1998].

2.5. Global Source Location

Given the bearing to the event and the range from the wave impedance comparisons, the source can be uniquely located on the Earth. To calculate the bearing to the event, the standard crossed-loop method was used. A best fit line can be plotted from the Lissajous pattern that is traced out when the two orthogonal magnetic field components are plotted on an x - y plot. This line is perpendicular to the actual great circle bearing to the event. The 180° ambiguity is resolved by calculating the measured Poynting vector, $\vec{E} \times \vec{H}$, which points away from the source on this great circle.

2.6. Calculating the Charge Moment

Given the source distance θ , the electric and magnetic spectra for the recorded event can then be compared with the theoretical spectra (equations (3) and (4)) to estimate the source current moment. In fact, if the recorded complex spectrum is divided by the theoretical complex spectrum (with a hypothetical white-noise source), the result is the frequency spectrum of the source current, $I(f) dS$.

This creates a few complications. Division by the theoretical spectrum is division by the system response in amplitude and phase. The system response has band edges at 3 and 120 Hz and a deep notch at 60 Hz. Inverting this would effectively divide by zero in several places, producing incorrect values for these frequencies, which were effectively lost when they were filtered out. Thus, instead of dividing by the theoretical spectrum, the recorded spectrum is multiplied by a modified version of the theoretical spectrum so that the resulting $I(f) dS$ is still zero in the frequency ranges where there is no information. These modified spectra can be interpreted as the inverse of the theoretical spectrum with the frequencies outside of the band edges and near the 60 Hz notch zeroed out. The effect of the constant background Schumann resonances, which effectively lower the signal-to-noise ratio of the recorded spectra, is ignored. Although in principle the charge moment is extractable from either the electric or magnetic field (following equations (3) and (4)),

in practice the magnetic field has been used because of its more accurate calibration.

2.6.1. Direct integration of the current moment. Given the frequency spectrum of the current, the vertical charge moment involved in the ground flash can be calculated by several methods. The most straightforward method is to assume a charge height dS (horizontal charge transfers do not excite a uniform Earth-ionosphere cavity) and then integrate the time series of the current to estimate the charge transferred.

Note that in the normal mode equations the current $I(t)$ is not provided but rather the current moment, $I(t) dS$. The latter quantity is divided by a height of 5 km for the channel length of the lightning resulting in the actual current. This height is based on observations of the height of the dominant positive charge layer in mesoscale convective systems [Marshall et al., 1996; Shepherd et al., 1996; Williams, 1998].

It is important to note that this method is accurate only if all frequencies of the current moment spectrum are available. Since the timescale of lightning processes can be microseconds, a very wide bandwidth is needed to avoid loss of information about the waveform. Because the actual bandwidth of our system extends only to ~ 120 Hz, all the information is lost about the actual current waveform at higher frequencies, which distorts the derived time waveform and affects the integration. For this reason, efforts to calculate the charge transfer without needing the extended bandwidth information (i.e., by working in the frequency domain) have also been pursued.

2.6.2. Impulsive estimate of the charge moment. The second method is to determine the charge transfer directly from the normal mode equations. Assuming a crude model of lightning current as an exponential form in the time domain [Sentman, 1996],

$$I(t) dS = I_0 ds e^{-t/\tau} [A \cdot m], \quad (10)$$

transforming to the frequency domain and letting τ go to zero,

$$\begin{aligned} I(f) dS &= \frac{I_0 ds}{j2\pi f + 1/\tau} \\ &= \frac{I_0 ds \tau}{j2\pi f \tau + 1} \\ &= I_0 ds \tau \quad (\text{for } 2\pi f \ll 1/\tau) \\ &= Q dS [C \cdot m], \end{aligned} \quad (11)$$

the charge moment $Q dS$ is derived from the current moment $I(f) dS$. As τ gets very short, the frequency spectrum of the current becomes nearly flat (since as $\tau \rightarrow 0$, the time waveform approaches a delta function if $Q = I_0 \tau$ is held constant). For time constants short in comparison with Schumann resonance timescales, $I(f) dS$ can be replaced in the normal mode equations with $Q dS$. Given this condition, the frequency spectrum $I(f) dS$ can also be viewed as a direct measure of the amount of charge transferred (any point on the graph gives an estimate of $Q dS$). Fortunately, the timescales of Schumann resonances (characterized by the time light takes to travel around the world) are long com-

pared to most lightning processes. The exception to this rule is the long continuing current which is an important aspect of this study.

For an exponential current waveform with a finite time constant, this method will also systematically underestimate the amount of charge transferred. This can be shown by using a well-known property of the Fourier transform,

$$X(0) = \int x(t) dt, \quad (12)$$

which states that the integral of the time domain waveform is the value of the frequency spectrum at $f = 0$. Since the Fourier transform of an exponential has its maximum magnitude at $f = 0$ (from equation (11)), the value at any other frequency will be lower and will produce a lower value for the charge moment. So the only usable frequency that will not underestimate the amount of charge transferred is the DC value ($f = 0$), which is outside of the system band pass.

An important feature of the impulsive estimation for the charge transfer is its independence of the system bandwidth, unlike the time-domain integration. The impulsive estimation is also not dependent on the assumption that the time-domain waveform for the current is exponential. Any waveform characterized by a time scaling parameter and which will cause the function to converge to a delta function in the limit of very small timescales is a permissible representation. The measurement is insensitive to waveform shape in this limit.

2.6.3. Charge moment and time constant estimates assuming an exponential current. A third method to determine the moment change retains the assumption of an exponential current but does not rely on either extended bandwidth or a short time constant. This method should be accurate if the lightning current conforms approximately to a simple exponential decay and if the current source spectrum is not wider than the recording bandwidth.

Returning to the Fourier transform of the exponential time waveform in (10), if the squared magnitude of the current spectrum (where $A = I_0 dS$) is inverted, the result is

$$\frac{1}{|I(f) dS|^2} = \left(\frac{2\pi}{A}\right)^2 f^2 + \left(\frac{1}{A\tau}\right)^2, \quad (13)$$

with f^2 as the independent variable [Huang, 1998]. Equation (13) can then be rewritten as

$$y = mx + b, \quad (14)$$

where we define

$$x = f^2, \quad (15)$$

$$y = \frac{1}{|I(f) dS|^2}, \quad (16)$$

$$m = \left(\frac{2\pi}{A}\right)^2, \quad (17)$$

$$b = \left(\frac{1}{A\tau}\right)^2 = \left(\frac{1}{I_0\tau dS}\right)^2 = \frac{1}{(Q dS)^2}. \quad (18)$$

If an unknown recorded spectrum is squared in magnitude and the reciprocal of the resulting graph is plotted as a function of f^2 , the outcome is a graph that is similar to (14). A linear least squares line can then be fitted to the graph. From the slope m of this line, the amplitude of the original waveform is obtained from (17):

$$I_0 dS = A = \frac{2\pi}{\sqrt{m}} [A \cdot m]. \quad (19)$$

By using (17) and (18), the time constant for charge transfer can be obtained:

$$\tau = \frac{1}{2\pi} \sqrt{\frac{m}{b}} [s]. \quad (20)$$

To find the parameters of the current moment time waveform, the inverse of the squared magnitude of the frequency spectrum is graphed against the squared frequency. The parameters of a linear least squares line are then calculated, and (19) and (20) are used to get the amplitude and time constant for the time waveform. Finally, the amplitude and time constant are multiplied to obtain the charge moment. Note that from (18), the y intercept b is the reciprocal of the square of the charge moment. Thus the amount of charge transferred can be obtained directly from the value of the best fit line at $f = 0$.

3. The Storm and The Measurements

3.1. Mesoscale Convective System

The majority of measurements discussed in this paper were obtained from one large mesoscale convective system (MCS) in the central United States. During the late afternoon of July 23, 1996, isolated convective storms (some severe) developed along the Colorado Front Range. During the early evening these clusters of storms merged into a larger-scale MCS, which then moved into southeastern Colorado and eastern Kansas. After local midnight (0600 UTC, July 24, 1996) the convection organized into a classic bow echo MCS while moving through the Texas-Oklahoma panhandle (as shown in the GOES satellite image in Figure 4).

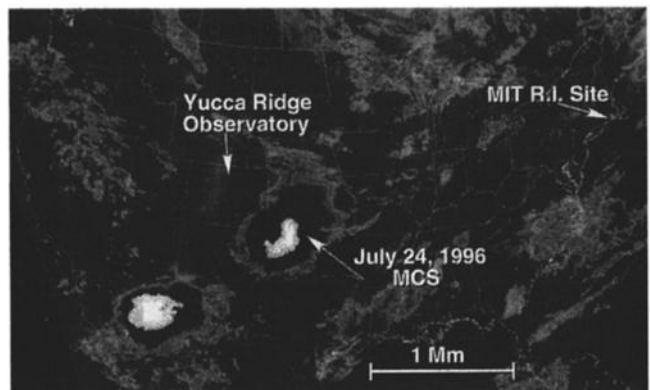


Figure 4. GOES infrared image of the July 24, 1996, Mesoscale Convective System (MCS) over Kansas and Oklahoma (0702 UTC). MIT RI, Massachusetts Institute of Technology, Rhode Island.

The storm at its peak had a radar areal coverage of 65,000 km². Between 0000 and 1200 UTC the NLDN recorded 85,900 strokes for a limited area which contained most of the MCS, of which 5.2% were positive. The highest overall flash rate occurred around 0700 UTC. The average -CG peak current was 21 kA while the +CGs averaged 31 kA during this period.

3.2. Massachusetts Institute of Technology Recording Station (Rhode Island)

The electric and magnetic field transients were continuously recorded at the Massachusetts Institute of Technology (MIT) field station in West Greenwich, Rhode Island [Heckman *et al.*, 1998], throughout the period of the July 24, 1996, storm. The satellite picture in Figure 4 shows that the region around the field station was clear of convective weather, which facilitated observations of the relatively isolated storm southeast of the Yucca Ridge station discussed in section 3.3. The recording station is located at 41.62°N latitude and 71.73°W longitude in a woods ~5 km from the nearest major highway.

The recording equipment consists of a ball antenna and two perpendicular magnetic coils. The vertical electric field is measured using Polk's [1982] original antenna, which consists of a spherical electrode with a radius of 15 inches on a 10 m pole [Keefe *et al.*, 1973]. The electric field signal from the antenna passes through a preamplifier housed inside the sphere and then through 600 feet of shielded twisted-pair cable to an amplifier with a notch filter at 60 Hz housed in an equipment shelter.

The two magnetic coils are identical in configuration, each 7 feet long and 3 inches in diameter with permalloy cores and 30,000 turns of wire. The coils are aligned with the geographic north-south and east-west axes, buried in trenches, and immobilized with sand bags. The coils are encased in 6 inch diameter PVC pipe helically wound with 210 turns of wire to form excitation coils for calibration. These calibration coils extend past the ends of the magnetometer coils such that the magnetic fields detected by the coil from the solenoid are uniform to within 1%. These signals are routed in the same fashion as the electric field signals to an amplifier and notch filters at 60 and 120 Hz in the equipment shelter.

Two computers each record digitized data from three analog channels, two for the magnetic field and one for the electric field. One computer records continuously and averages multiple spectra to record the background Schumann resonances [Heckman *et al.*, 1998]. The other machine records the transients which exceed a preset threshold in the azimuthal magnetic field above the background resonances. The usual magnetic power (amplitude) threshold for the 120 Hz band pass is $\sqrt{(H_{ns}^2 + H_{ew}^2)/2} = 11.6 \mu\text{A/m}$.

The amplitude and phase response of the sensors are essential for extracting information on lightning currents. For the electric sensor the phase response is obtained with an auxiliary excitation electrode placed in close proximity to the spherical electrode, which can be lowered for access on

the ground [Polk, 1982]. The complete amplitude and phase response of the magnetic coils is measured with the external solenoidal coils.

To provide accurate time stamps for the electromagnetic data, a Global Positioning System (GPS) antenna is used. These time stamps provide absolute millisecond time resolution of events, which allows comparisons with other recording stations and data sets, most notably from the National Lightning Detection Network. The current method used to clock events is a major improvement over that available in the earlier study [Boccippio *et al.*, 1995].

3.3. Yucca Ridge Observations (Colorado)

3.3.1. Video observation of sprites and elves. At the Yucca Ridge Field Station (YRFS) located near Fort Collins, Colorado (40.67°N, 104.93°W), the SPRITES'96 field campaign obtained low-light television (LLTV) measurements of sprite and elve events time-stamped by GPS. These events occurred above High Plains MCSs. These measurements were used to determine the times of maximum sprite and elve intensity, which were compared with the return stroke times and the charge transferred in the positive ground flashes. During the time period (0300–0900 UTC) in which sprites were under continuous LLTV optical surveillance from the YRFS, a then record number of transient luminous events were detected, 245 sprites, 24 elves, and 35 elve-sprite combinations. The start times and durations for each event were logged from GPS time tagged video to within the 16.7 ms video field duration. The average peak currents were 61 kA for sprite +CGs, 107 kA for elve-sprite combinations, and 120 kA for pure elves. This was consistent with findings from past storms [Boccippio *et al.*, 1995; Lyons, 1996a]. Comparisons with Next Generation Weather Radar (NEXRAD) base reflectivity suggested that the vast majority of sprites and elves were associated with reflectivities of less than 40 dBZ. These events showed a clear tendency to avoid the high-reflectivity convective cores at the leading edge of the system and were clustered near the center and rear of the large trailing stratiform region. Analysis of regional composite radar reflectivity maps suggested that a radar "bright band" pattern may have been the feature to which the sprites and perhaps elves were most closely associated [Nelson, 1997].

3.3.2. Brightness measurements of sprite events. For the SPRITES '96 campaign, Utah State University operated three cameras from the Yucca Ridge Field Station: a solid-state bare CCD imager and two intensified Isocon video cameras. The measurements of the same events on July 24, 1996, documented with ELF methods, enabled comparisons of the lightning charge moment and relative sprite brightness over the full range of source excitation strengths. All three optical instruments were coaligned and mounted on an electronically steerable alt-azimuth tripod providing pointing information to an accuracy of ~1°. The fields of view of the cameras were all relatively small (20°–30°), and the Yucca Ridge patrol cameras provided azimuthal data on potential sprite storms. The CCD system utilized a large area 1024

x 1024 pixels CCD array (6.45 cm²) of high quantum efficiency (~80% at 650 nm). This system was originally developed for airglow imaging studies [e.g., *Taylor and Pendleton*, 1996] and was adapted for sprite studies by fitting it with a narrow angle (~17° diagonal) telecentric optical arrangement, permitting high spatial resolution, “monochromatic” images of sprites over a small area of sky. The primary sprite emissions studies were the N2 first positive band emissions at 665 and 886 nm (identified by *Mende et al.* [1995] and *Hampton et al.* [1996]) and the N2 first negative emission at 427.8 nm [*Armstrong et al.*, 1998]. High transmission (>75%) interference filters incorporating a high off-band-blocking factor of 10⁻⁵ from 200 to 1100 nm were used to isolate these emissions. The central wavelengths and the full-width half maximum (FWHM) bandwidths of the three filters used were 665.5 nm (bandwidth 28.2 nm), 888.7 nm (12.7 nm) and 427.9 nm (3.0 nm). A computer-controlled filter wheel was used to select the emission of interest.

For the SPRITES '96 campaign the majority of measurements focused on the N2 first positive emission at 665 nm, and the CCD imager recorded over 100 sprites. The data were binned on chip to 512 x 512 pixels and digitized to 16 bit resolution prior to storage (~0.5 megabytes per image). To maximize the probability of capturing a sprite, the camera shutter was held open for 20 s, and the data was downloaded to disk in the following ~10 s. In this manner, high-resolution, spectrally resolved “snapshot” images of sprites were obtained. In parallel with these measurements the two intensified Isocon video cameras were used to provide additional data on the sprite events. One camera (field of view ~22°) was fitted with an identical red 665 nm filter while the other (field of view ~28°) was unfiltered and recorded the sprites in white light. Both of these imagers had a frame rate of 50 Hz, providing a timing resolution of 20 ms [*Taylor and Clark*, 1996].

The CCD data have been analyzed to determine the relative brightness and brightness variability of the sprites observed during this campaign. The high stability and dynamic range of the detector provide an excellent capability for this study, which indicates a very large range of brightnesses.

To enable a quantitative comparison of sprites observed at various look directions and in different regions of the image plane, the data were first “flat fielded” to remove lens vignetting and line of sight effects. This is a well-established technique that is regularly used in airglow studies [e.g., *Garcia et al.*, 1997] and that was achieved by summing together several (typically 10) images centered on the data image to obtain an average image, which was then used to normalize the sprite data. Measurements of the peak brightness associated with each sprite were then made by investigating the pixel levels within the sprite structure. To eliminate the contributions of stars occurring within the sprite, several adjacent pixel values were summed together to determine an average peak value. Finally, to take account of the differing sky backgrounds from night to night and as a function of elevation and time, an area of sky adjacent to the sprite (but free from stars and other optical emissions) was sampled and

subtracted from the sprite signal to provide an accurate (~5–10% depending on signal level) measure of the true sprite signal for the relative brightness studies to be discussed in section 4.4.

4. Results of Measurements

4.1. Sample ELF Event Analyses for a Sprite and an Elve

Selected ELF observations for positive ground flashes associated with an elve and a sprite observed from Yucca Ridge over the July 24, 1996, storm are shown in Figures 5 and 6, respectively. Multiple plots are included here to illustrate the use of Schumann resonance observations in characterizing events and to draw attention to fundamental distinctions between elve and sprite events. Both Figure 5 and Figure 6 consist of eight plots: the raw electric and total magnetic time series for the transient event (Figures 5a, 5b, 6a, and 6b), the Lissajous plot representing the transient in the two components of magnetic field over the same time interval shown in the individual transients (Figures 5c and 6c), the wave impedance spectrum for which the event distance from the Rhode Island station is obtained (solid curve in Figures 5d and 6d) and the theoretical wave impedance for an event at the location specified by the NLDN (dashed curve in Figures 5d and 6d), the electric and magnetic frequency spectra (solid curves in Figures 5e, 5f, 6e, and 6f) and the same theoretical spectra for an impulsive source at the NLDN location (dashed curve in Figures 5e, 5f, 6e, and 6f), the frequency spectrum of the current moment derived from the magnetic field measurements and the normal mode equations (Figures 5g and 6g), and finally the current moment in the time domain (Figures 5h and 6h).

Salient features of the plots for the elve and the sprite events in Figures 5 and 6, respectively, are discussed here in parallel. In the electric field time series both events commence with strong negative excursions, indicative (in our electronics convention) of positive charge transfer from cloud to ground. The initial positive excursions in H_ϕ in both records are consistent with downward electric current, thereby providing self-consistency with the recorded E_z . Greater low-frequency content is already apparent in the sprite-related waveforms in contrast to the elve case.

The magnetic Lissajous patterns (Figures 5c and 6c) in both cases exhibit significant departures from the clean linear form expected for a vertical current source in a uniform waveguide. This departure limits the absolute accuracy in great circle bearing to several degrees.

Reasonable agreement is observed between theory (based on the NLDN location of the return stroke channel of the +CG) and measurement in the case of wave impedance. The difference at the high end of the frequency range is due to the 60 Hz notch filter. The difference at low frequencies in both cases is less well understood. In the elve case the range was 2.86 Mm, with a difference between the ELF- and NLDN-determined range of 150 km (~7% of the total range in megameters). In the sprite case the distance was 2.32 Mm,

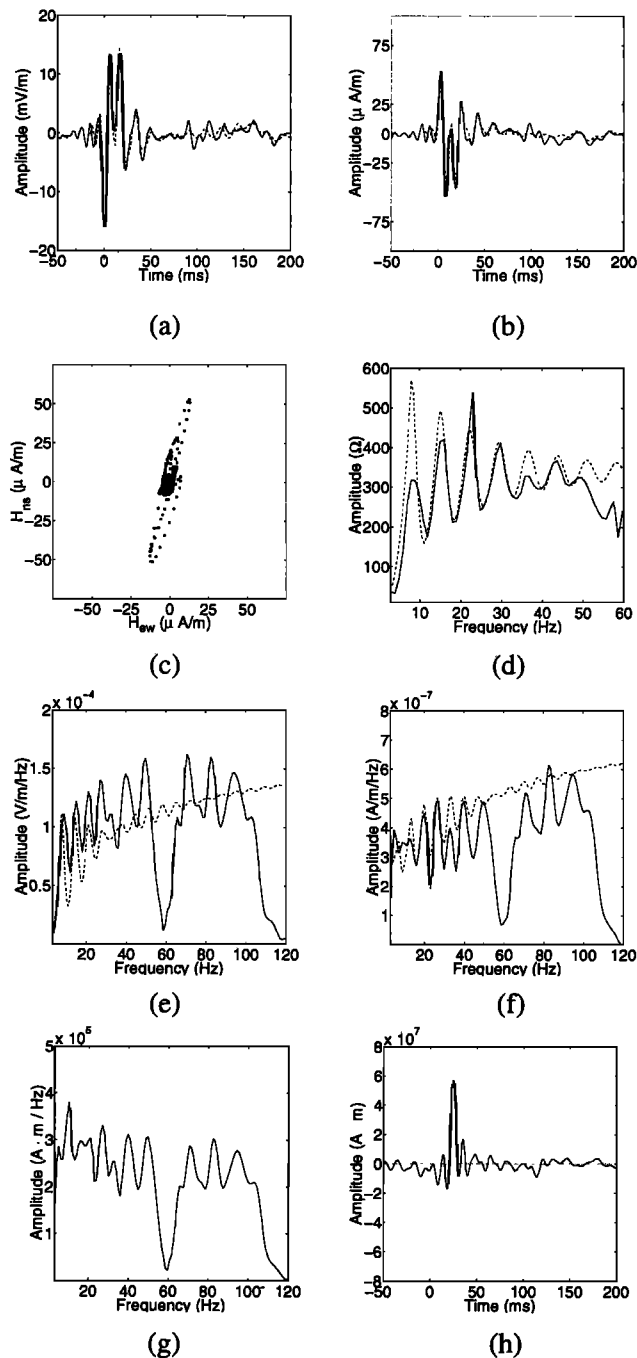


Figure 5. Analysis of sample elve event which occurred at 0452:19.531 UTC (dashed curves are for theory) at a range of 2.86 Mm: (a) electric time series, (b) magnetic time series, (c) magnetic bearing Lissajous, (d) wave impedance spectrum, (e) electric spectrum, (f) magnetic spectrum, (g) $I(f) dS$ spectrum, and (h) $I(t) dS$ estimate.

with a range error of 280 km. The reason for the systematic errors in range is not well understood at present. The distance error does not cause ambiguity in the identification of these exceptional positive events; the GPS timing used in both the NLDN and ELF data confirms the event identification in nearly every case for the North American analysis.

The normal mode structure evident in both the electric and magnetic frequency spectra, with well-defined peaks at spe-

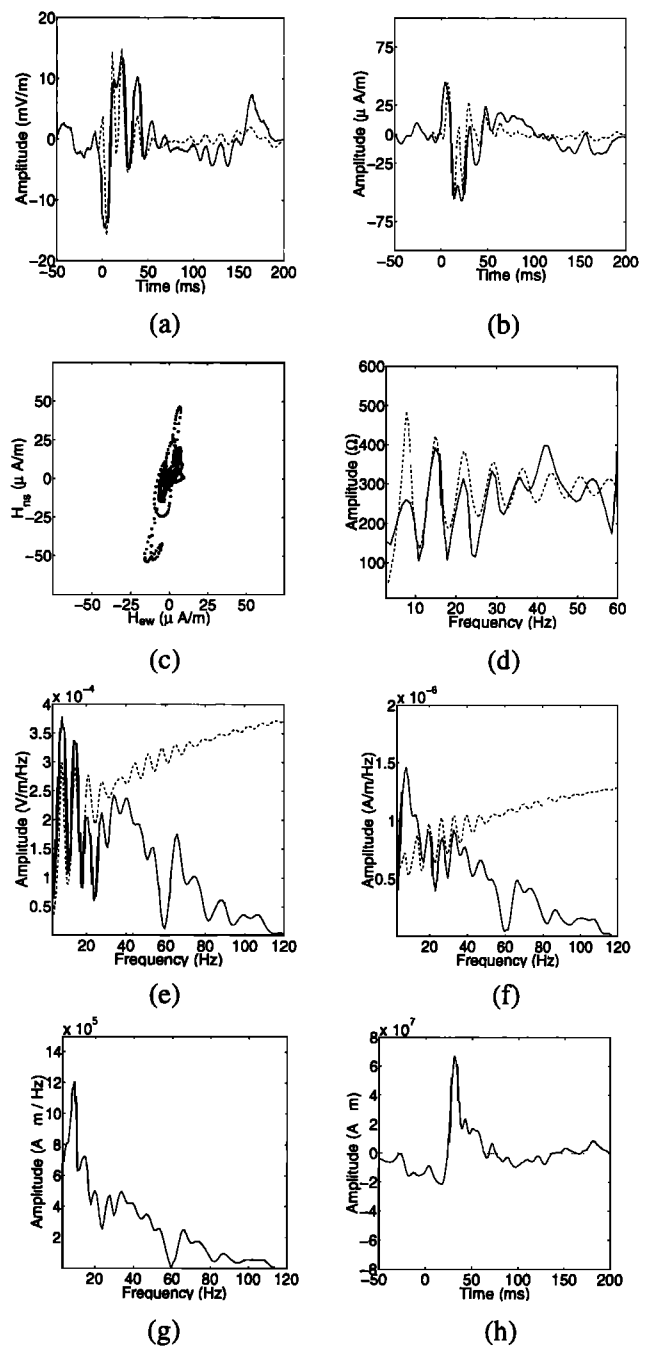


Figure 6. Analysis of sample sprite event which occurred at 0345:25.695 UTC (dashed curves are for theory) at a range of 2.32 Mm: (a) electric time series, (b) magnetic time series, (c) magnetic bearing Lissajous, (d) wave impedance spectrum, (e) electric spectrum, (f) magnetic spectrum, (g) $I(f) dS$ spectrum, and (h) $I(t) dS$ estimate.

cific frequencies (near 8, 14, 20, 26 Hz, etc.), verify that these positive ground flashes are single-handedly ringing the Earth-ionosphere cavity, as noted earlier by *Boccippio et al.* [1995] for flashes associated with sprites. The distinctly different trends with frequency in the case of the elve and the sprite underscore the distinction between an impulsive white-noise source (elve) and a "red"-noise source (sprite). The theoretical (dashed) curves pertain to delta function cur-

rent sources. The trends in theory and experiment for the elve event are similar, but marked departures are evident in the sprite case, which has the prominent enhancement of the fundamental 8 Hz mode which defines the classical Q burst [Ogawa *et al.*, 1967].

The frequency spectra for the current moment (Figures 5g and 6g) and the current moment itself (Figures 5h and 6h) confirm this distinction. The spectrum for the elve event is only slightly “pink” whereas the spectrum for the sprite is decidedly red. The extracted waveforms for current moment, substantially impacted by the limited 120 Hz bandwidth of the ELF measurements, are nonetheless substantially different, with strong evidence in the sprite case for the extended tail lasting for tens of milliseconds, the long continuing current.

4.2. Moment Changes and Time Constants for Charge Transfer

A histogram of the derived charge moments (from the impulsive estimate using only the 8 Hz mode) for the July 24 sprite and elve events is shown in Figures 7a and 7b. We have also recently integrated the charge moment calculations in an automated program for transient analysis, which would provide statistics on large numbers of events. The recorded transient data from July 13 to July 31, 1997 were run through the new analysis program, and Figures 8a–8d show the distribution of the calculated charge moments. We see that there are more positive events than negative events and that the positive distribution has a larger part of its population above

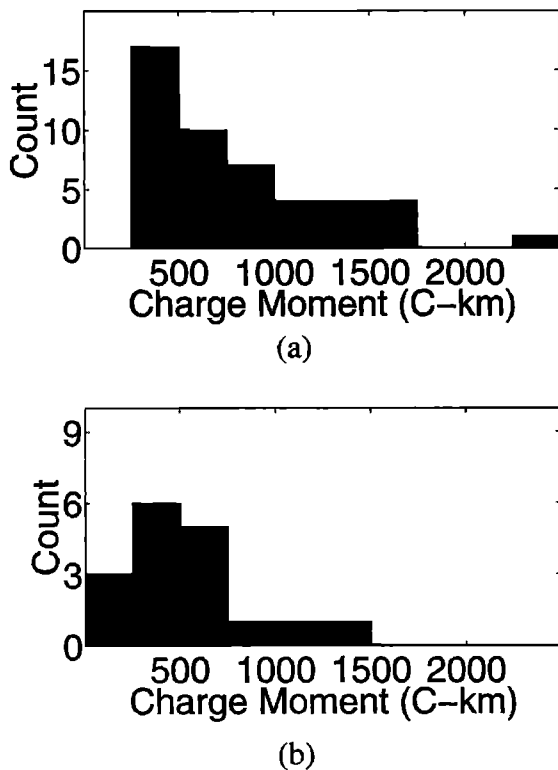


Figure 7. Charge moments ($Q dS$) by the impulsive assumption for July 24, 1996, events for (a) sprites and (b) elves.

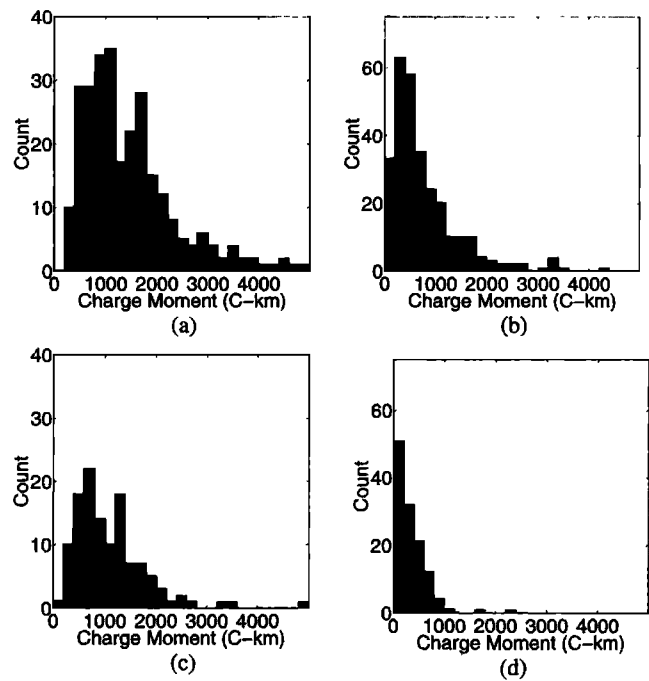


Figure 8. July, 1997, charge moments ($Q dS$): (a) positive events by waveform integration, (b) positive events by the impulsive assumption, (c) negative events by waveform integration, (d) negative events by the impulse assumption.

the $Q dS = 300$ C-km threshold (which we hypothesize is the cutoff for sprite formation) than the negative distribution does. We do see some of the impulsive negative events above the 300 C-km level, which means, in theory, that there could have been sprites associated with them or that they all occurred within a certain time (an unusual storm, for instance). However, upon closer examination of these large charge moment negatives, we see no real distinguishable pattern to their time or location.

For all of the sprite and elve events for the July 24, 1996, data set, the frequency spectrum of an exponential time waveform was fitted to the frequency spectrum for each event, and the proper parameters were extracted. The histograms of the derived time constants and charge moments are shown in Figures 9a and 9c and Figures 9b and 9d, respectively. The average time constant is 5.4 ms for the sprite events, and 3.6 ms for the elve events.

As a check on the validity and consistency of our different methods for determining the charge moment, we plot our methods against each other to reveal systematic variations. Figure 10 compares the results of the three methods (impulsive, exponential, and integrated) used in this study to estimate the charge moment ($Q dS$). We can see from Figure 10 that the three estimates for the charge moments show good correlation with each other. The exponential fits and the impulsive estimate match very well, and the integration of the derived current time waveform (even though a systematic multiplicative offset is apparent) produces moments which are well correlated with the other two methods, assuring self-consistency in the three charge moment estimators.

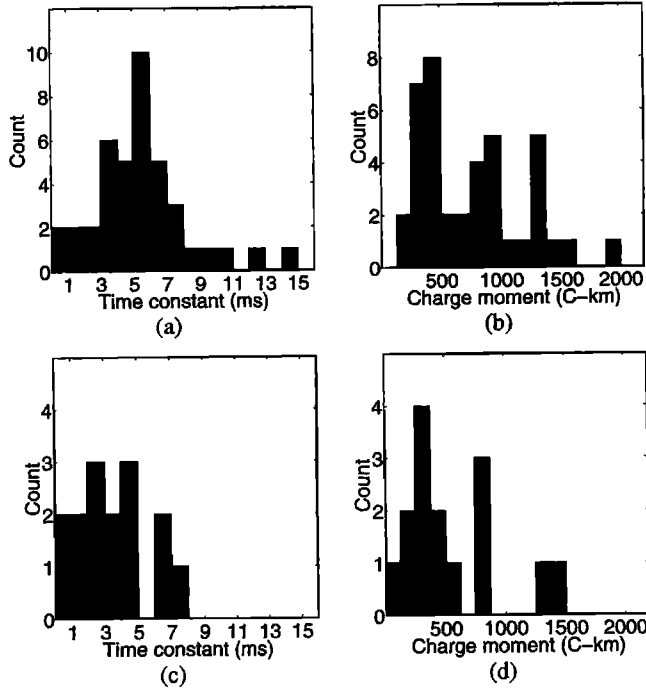


Figure 9. Derived time constants and charge moments ($Q dS$) and for July 24, 1996, events: (a) time constants for sprite-producing positive ground flashes, (b) charge moments for sprite-producing positive ground flashes, (c) time constants for elve-producing positive ground flashes, and (d) charge moments for elve-producing positive ground flashes.

4.3. Sprite and Elve Time Lags From the Positive Return Stroke

The Xybyon LLTV observations of sprites and elves from Yucca Ridge were carefully examined after the fact for absolute timing relative to the NLDN return stroke time. The brightest field (integration time of 16.7 ms) of a two-field video frame (integration time of 33.3 ms) was identified for each optical event, and its midpoint was tabulated as the most closely resolved time for that event. In the case of elves the event occupied only a single field whereas for sprites the events were sustained for an average of four fields (and occasionally for 10 fields), though typically one field clearly dominated. Times for events on July 24, 1996, were compared with absolutely timed return strokes for NLDN ground flashes and the list of absolute arrival times for transient events in West Greenwich, Rhode Island. On the basis of these comparisons, NLDN return stroke times were paired with the elves and sprites. The LLTV times were adjusted for the light delay from the MCS location to Yucca Ridge (~2 ms).

Histograms of time lags (LLTV time minus NLDN time) for sprites and elves are shown in Figures 11a and 11b, respectively. The lags for the elve events are close to zero on this coarsely resolved timescale, whereas systematic delays, on average, are observed for the sprites.

4.4. Lightning Charge Moment and the Corresponding Relative Sprite Brightness

The relative brightnesses of 24 sprites were determined, of which the parent positive ground flashes from 22 of 24

of these events triggered the Rhode Island ELF system. Of these 22 triggers, only 7 processed satisfactorily to derive charge moments. The charge moments in this case were extracted from the current moment frequency spectrum at a frequency of 8 Hz. These seven points are plotted in Figure 12. The relative sprite brightness (on a verified linear scale of brightness) varied from “faint” (3000 counts) for the dimmest sprite to “very bright” (>19,300 counts) for the brightest sprite included in Figure 12. Five of the seven points are seen to follow the dashed line in Figure 12, indicating a clear positive correlation between the charge moment and sprite brightness.

5. Discussion

5.1. Comparison Among Methods for Charge Moment Estimation

The exponential fit method that we use to find the parameters of a lightning event assuming an exponential time waveform is similar to the exponential fits of *Burke and Jones* [1996]. These authors found time constants that ranged from 12 to 50 ms for positive events and from 17 to 36 ms for negative events. They also obtained an average charge moment ($2Q dS$) of 3300 C-km for positive events and 1500 C-km for negative events. These mean values are similar to the present results, but the time constants are much longer. It is important to note, however, that our calculations are being made for the sprite-producing events of a single day for a

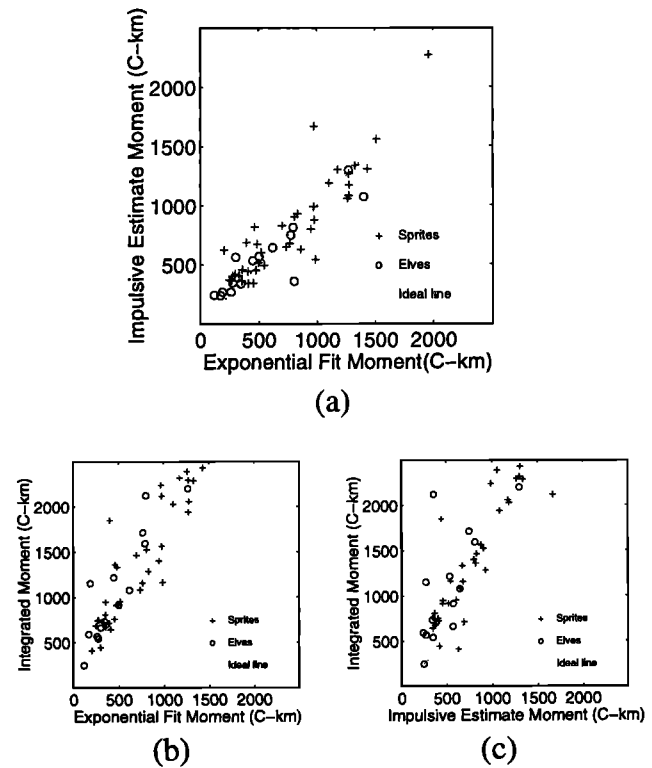


Figure 10. Comparison of charge moment ($Q dS$) estimates for July 24, 1996, events: (a) exponential versus impulsive, (b) exponential versus integrated, and (c) impulsive versus integrated.

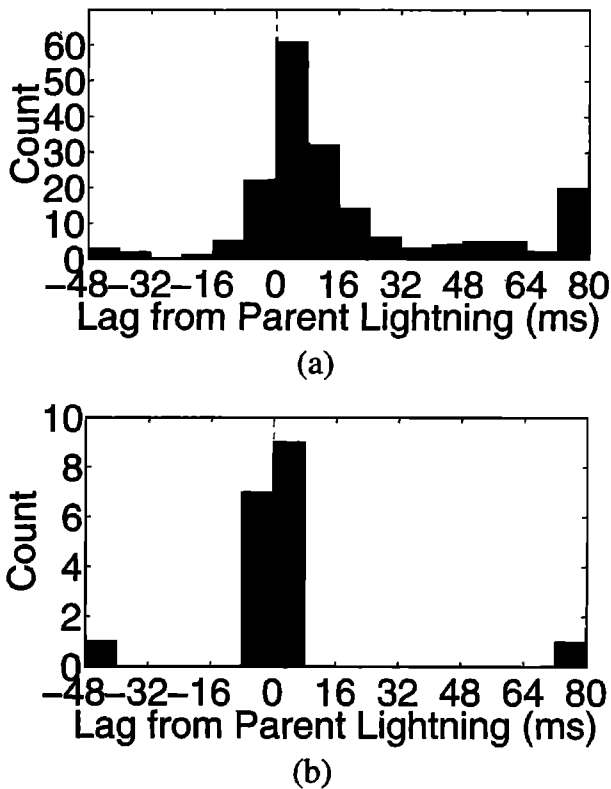


Figure 11. Time lags between the return stroke of parent lightning and (a) sprite events and (b) elve events.

storm in North America, while their calculations were made for the largest events they could find globally, so the results do not necessarily directly compare.

The discrepancies in time constants may be the result of the difference in system band pass of the two experiments. *Burke and Jones's* [1996] equipment had a band pass up to only 45 Hz, while ours extends to 120 Hz. Although we both modeled the lightning current as an exponential, it should be noted that this is an oversimplified model for lightning current. At the very least, the current decay of the lightning stroke should be modeled as a two-timescale waveform [Pierce, 1977], with a large-amplitude, fast decaying component, followed by a smaller-amplitude component with a much longer time constant. This would be a better approximation to what has been observed for the current waveforms of these lightning strokes.

Given such a two-time constant model for a lightning stroke, because *Burke and Jones* [1996] has a much narrower bandwidth, the fast decaying component would be less dominant in the recorded waveform. Their exponential fits would then tend to try and fit to the more slowly decaying component, which would lead to larger time constants. Our bandwidth, on the other hand, might be large enough that the fast decaying component is not greatly distorted by the band pass, and so it would dominate the waveform that we receive. Thus our exponential fits would tend to fit the faster component, leading to smaller time constants.

Cummer et al. [1998] use a method not relying on the cavity resonances to estimate the charge moment, primarily be-

cause their system bandwidth starts at 24 kHz and extends down to 15 Hz. The sprite charge moments are estimated by fitting the recorded sferic waveforms to a model to obtain the current waveform, which they can then integrate. Fortunately, we also have measurement and analysis for two of the four events analyzed by *Cummer et al.* from the same July 24, 1996, storm.

For the first event at 0409:19.553 UTC their calculated charge transfer is 325 C. Given their assumed 10 km height the charge moment ($Q dS$) is 3250 C-km. For comparison we obtain 3000 C-km from the impulsive estimate (8 Hz only) and 2400 C-km from the integration. The exponential fit does not provide an estimate in this case because the best fit line to the inverted current spectrum (section 2.6.3) does not have the required slope to produce a positive (and real) charge moment estimate. This result may be due to significant departures of the current waveform from an exponential. The value for the impulsive estimate is quite close to *Stanford's* values, but the integrated number is too low.

The second event is at 0512:20.345 UTC. They calculated the amount of charge to be 145 C, which translates to a moment ($Q dS$) of 1450 C-km. Our impulsive moment estimate is 2000 C-km, with an integrated estimate of 2300 C-km. The exponential fit for this event gives a moment estimate of 1200 C-km. In this case the exponential estimate is fairly close, and the impulsive and integrated estimates are both too high.

5.2. NLDN Peak Current as an Indicator of Charge Moment for Positive Ground Flashes

As stated in section 1, a large NLDN peak current for positive ground flashes has often been considered as an indicator of sprite production [*Boccippio et al.*, 1995; *Lyons et al.*, 1998]. We see, however, in Figure 13 that very large NLDN peak currents are associated with elves rather than

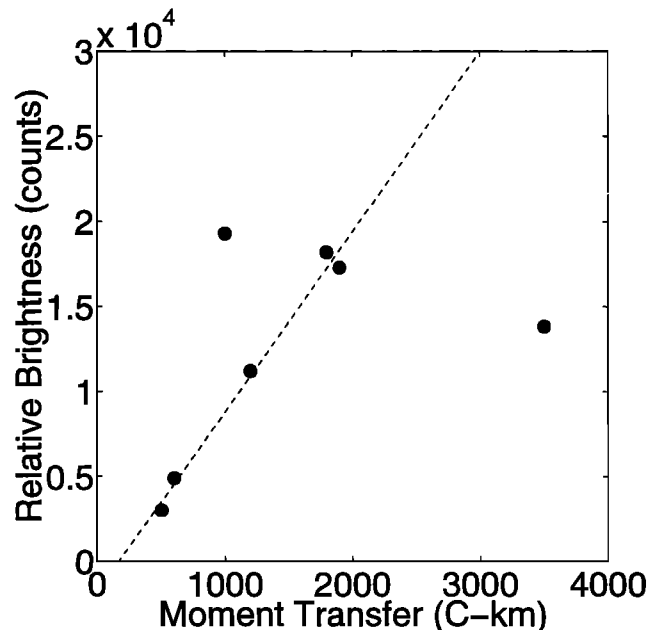


Figure 12. Relative brightness versus charge moment ($Q dS$) for sprite events.

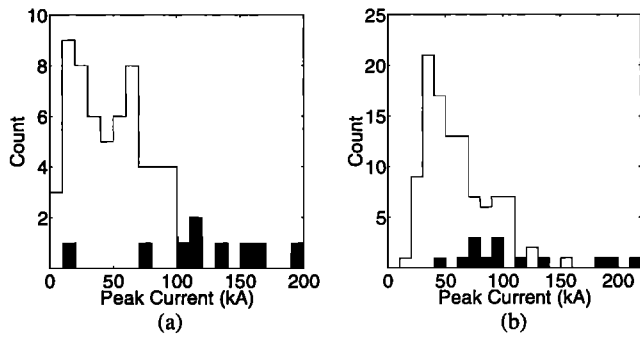


Figure 13. Positive peak currents (recorded by the NLDN) associated with sprite (open) and elve (solid) events for (a) July 25, 1995, and (b) July 24, 1996.

with sprites, consistent with the idea that elves are caused by the radiation (EMP) field rather than the electrostatic field of the lightning. It has also been shown that the charge moment is the relevant quantity in assessing mesospheric breakdown in the Wilson diagram (Figure 2). Furthermore, comparisons in Figure 12 support the importance of charge moment in determining sprite brightness.

The value of the NLDN peak current as a diagnostic for sprites is tested in Figure 14, where values for ELF-measured charge moment and NLDN peak current are plotted for numerous positive CGs in the July 24, 1996, storm. Little correlation is observed. This lack of correlation is attributed to the understanding that peak return stroke currents are related primarily to the charge deposited on the leader channel and to the observation that the majority of charge transfer in most positive ground flashes is transferred by the continuing current rather than by the return stroke. Since NLDN peak current can be a misleading indicator for sprite production, charge moments determined by wideband ELF measurements are preferable diagnostics.

5.3. ELF Characteristics of Transients Associated With Sprites and Elves

Positive ground flashes that produce sprites and elves have been identified as strong exciters of the Earth-ionosphere waveguide. Distinct differences in the lightning source characteristics appear to reflect the differences in optical characteristics noted in other studies [Fukunishi et al., 1996; Lyons, 1996b; Watanabe, 1999].

The elve lightning is of short duration in comparison to that associated with sprites. This conclusion is supported by the time constant analysis (Figures 9a and 9c) and the tendency for current spectra to be largely independent of frequency (e.g., Figure 5g). The recording bandwidth of 120 Hz is not adequate to resolve the initial high-frequency components of these events, including the return stroke and the fast recovery therefrom. The NLDN bandwidth (5–500 kHz) is better suited here, and these observations (Figure 13) clearly show that peak currents in the elve lightning events often exceed those associated with sprites. Despite these larger peak currents, the total charge transfers (assuming the height of the positive charge reservoir in the parent storm is the same for elve and sprite lightning) for elve

events are less, on average, than those for sprite events, as shown by the comparison of Figures 7a and 7b.

One unresolved issue with these observations is why some moment changes for elves are larger than the minimum value ($Q dS \approx 300$ C-km) for sprites. Why then did no sprite appear for these larger moment changes?

The larger lightning charge moments (and likely greater charge transfers) associated with sprite events in Figure 7a are attributable to the longer durations of the parent lightning currents. The time constants for the assumed exponential currents (Figure 9a) are longer, and the duration of the inferred currents is often several tens to a few hundred milliseconds (e.g., Figure 6h). The single time constant exponential form for these currents (equation (10)) is probably flawed, as noted in earlier studies [Burke and Jones, 1996; Cummer and Inan, 1997; Armstrong et al., 1998]. The large initial current in the submillisecond time frame, which is not well resolved with our limited recording bandwidth, may account for the charge transfer that initiates the sprite [Fukunishi et al., 1996], but the persistent charge transfer in the subsequent long continuing current may be essential for sustaining a notably weaker sprite luminosity for an average of three to five video fields (50–80 ms) [Lyons, 1996b]. Lightning durations are clearly critical in influencing overall ELF behavior.

As noted by Sentman [1996], when the duration of the lightning current is small in comparison to the Schumann resonance timescales (i.e., to the time required for light to travel round the Earth-ionosphere cavity, 125–140 ms), then the ELF current spectrum is white (i.e., independent of frequency). Ordinary return strokes with durations of hundreds of microseconds satisfy this condition best, but generally the charge moments are small on account of the short durations. These events do not stand out sufficiently against all the other lightning to be treated by the methods described

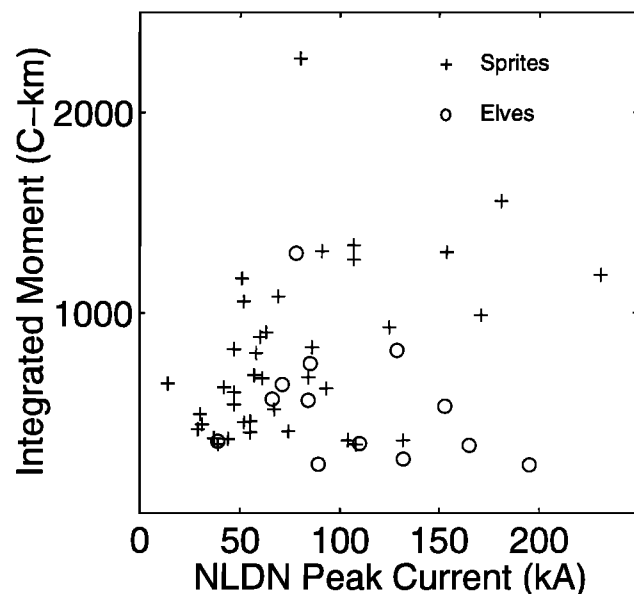


Figure 14. National Lightning Detection Network (NLDN) peak current versus impulsive moment estimate.

in this paper (section 2). For elve lightnings the durations may be an order of magnitude larger than ordinary negative return strokes (several milliseconds instead of several hundreds of microseconds) but still an order of magnitude smaller than Schumann resonance timescales. Hence the “white” (or slightly pink) frequency spectra characteristic for elves (Figure 5f). For sprites whose parent lightning often shows a long continuing current (Figure 6h), the current duration may be comparable to the positive half cycle of a resonant mode. When the duration of the current is in the range 30–60 ms, the fundamental 8 Hz resonant mode is preferentially excited, and the current source spectrum is preferentially enhanced at low frequencies, consistent with the observations described earlier in section 4.1.

ELF transient events with preferential energy in the lowest (8 Hz) resonant mode were named “Q bursts” by *Ogawa et al.* [1967], where “Q” connotes “quiet,” that is, transient disturbances which are relatively quiet at the higher frequencies in the Schumann resonance band. (This interpretation differs from that of *Sentman et al.* [1995] where the “Q” is linked with the quality factor of the Earth-ionosphere cavity). Since the time of *Ogawa et al.*’s definition, the term “Q-burst” has been applied nondiscriminantly to all ELF transients [e.g., *Sentman et al.*, 1995; *Burke and Jones*, 1996; *Nickolaenko*, 1997; *Yamamoto and Ogawa*, 1996], regardless of the frequency content of the events. In light of the evidence presented here for large transient events in the Earth-ionosphere waveguide that are not quiet in *Ogawa et al.*’s original sense, it is, perhaps, advisable to apply the Q burst nomenclature to only that special subclass of transients with a dominant 8 Hz component. The theoretical predictions for impulse excitations at small source-receiver distances (like the measurements within the North American continent reported here with 2–3 Mm source-receiver separations and illustrated in Figures 5f and 5f) should also be noted in this context: the power spectral density is actually increasing with frequency and so these events cannot be characterized as “quiet.” ELF transients with negative polarity are most likely to exhibit the latter behavior.

5.4. C.T.R. Wilson Diagram and Mesospheric Breakdown

Having presented measurements of lightning source moments associated with sprites and elves observed on July 24, 1996 in section 4.2, it is appropriate to return to the Wilson diagram introduced in section 2.1, illustrated in Figure 2, and repeated in Figure 15 for convenience. It is worth emphasizing that these predictions for air breakdown, regardless of process, are based purely on electrostatics with the following implicit assumptions: (1) the charge transfer in the parent lightning takes the form of a vertical dipole, (2) the multiple images associated with Earth and upper atmosphere conductors are ignored, and (3) the moment change is imposed by the lightning discharge in a time short in comparison with the local electrostatic relaxation time of the upper atmosphere (Figure 3). It is also important to note that the moment change we infer electromagnetically on the basis of normal mode equations is $Q dS$, whereas the electrostatic

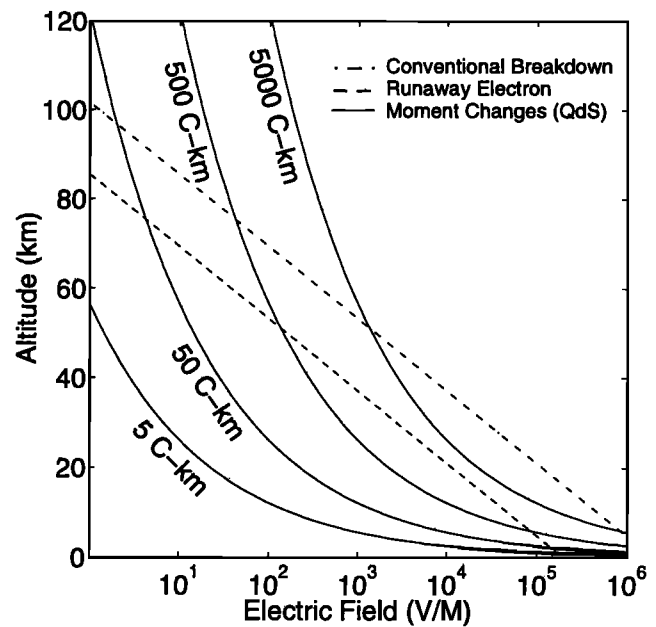


Figure 15. Breakdown electric field versus height and charge moment.

moment change associated with ground flashes is $2Q dS$ owing to the image charge in the Earth.

Regarding assumption 1, it is natural to question the validity of a compact charge source in the face of evidence that the positive charge reservoir with which sprites and elves are associated is both elevated and laterally extensive. The argument for an elevated source, in the 10–15 km altitude region for sprites, is not strongly supported [*Williams*, 1998] by available observations [e.g. *Krehbiel*, 1981; *Mazur et al.*, 1998], which indicate a laterally extensive positive charge reservoir in the 4–6 km altitude range. This height is only 10% of the altitude where sprites are believed to initiate, thereby substantiating a compact source in the vertical. Electrostatic models treating the horizontal extents of the charge reservoir have been considered by *P. Krehbiel* (personal communication, 1995) and *Marshall et al.* [1996]. These results demonstrate the capacity for charge accumulations substantially larger than those found in ordinary thunderstorms without dielectric breakdown in the troposphere. For a fixed total charge, the compact point dipole produces the largest vertical field along the dipole axis, but the differences with the extended source are not large unless the diameter of the source region is comparable with the height of the sprite. This latter condition may actually be satisfied in the stratiform precipitation region of large mesoscale convective systems [*Boccippio et al.*, 1995; *Williams*, 1998; *Mazur et al.*, 1998]. From this standpoint the predictions for fields in Figure 15 are the most favorable ones for breakdown given the assumed charge moments.

Regarding assumption 3 above, the validity of the electrostatic approximation can be judged by consideration of the timescales for charge transfer in large positive ground flashes and their comparison with the profile of electrostatic relaxation time in the upper atmosphere (Figure 3). Time

constants for charge transfer inferred from our ELF measurements were discussed in section 4.2. The characteristic timescales for charge transfer in large positive ground flashes have also been inferred from ELF observations (with different recording bandwidths) by *Burke and Jones* [1996] and *Cummer and Inan* [1997]. In light of the substantial differences among the ELF results (which may well be attributable to the different recording bandwidths), we have examined observations in the literature of large positive ground flashes by electrostatic methods on the ground and by optical methods from space. All of these results are summarized in Table 1. Unfortunately, it is not known whether these positive ground flashes produced sprites or elves, with the exception of the subset of the *Mitchell* [1997] optical observations for which both NLDN positive ground flashes and sprites were confirmed. With some exceptions the numbers are consistent with the idea that a substantial fraction of the charge transfer in positive flashes occurs in a time less than 10 ms, the relaxation time at an altitude of 50 km (Figure 3). This time frame is consistent with *Yucca Ridge LLTV* observations that the intense initial portion of the sprite often occurs within this time after the positive return stroke (Figure 6h) [*Fukunishi et al.*, 1996; *Bell et al.*, 1998]. These results, when taken with the information on relaxation time in Figure 3, support the use of simple electrostatic calculations on which the Wilson diagram is based.

Consideration is now given to the interpretation of the Wilson diagram for the entire range of moment change exhibited by lightning, from a few coulomb-kilometers to thou-

sands of coulomb-kilometers. The most prevalent lightning type is the small intracloud flash with vertical moment changes of the order of $Q dS = 10\text{--}20$ C-km [*Mackerras*, 1968; *Krehbiel*, 1981; *Krider*, 1989; *Koshak*, 1991, and personal communication, 1991]. According to Figure 15, conventional air breakdown would require an extreme initiation height of ~ 110 km. Here the electrostatic relaxation time (Figure 3) is submicrosecond, and any field is largely excluded. Electron runaway breakdown is likewise precluded because of the high altitude and short relaxation time. No mesospheric luminosity is expected to result from intracloud lightning of this kind.

The most prevalent ground flashes are of negative polarity with typical charge moment changes of order 100 C-km. Ordinary air breakdown at $Q dS = 95$ km is still precluded by the conductive *D* region of the ionosphere. Runaway breakdown is, however, a marginal possibility. According to the nighttime curve in Figure 3, the relaxation time at 75 km where the 100 C-km curve intersects the runaway breakdown line is a few milliseconds, which is longer than the usual times for charge transfer in the return stroke.

Positive ground flashes that appear to be causal to elves and documented in Figure 7 have measured moment changes which are 5–10 times greater than those for ordinary negative ground flashes. Although an electromagnetic (i.e., EMP) mechanism is widely preferred over an electrostatic mechanism for the origin of elves [*Krider*, 1994; *Inan et al.*, 1996b], it is of interest to examine the magnitude of the electrostatic stress in the altitude range exhibited by elves. In

Table 1. Time Constants for Transfer of Charge in Positive Ground Flashes in Other Studies

	Event	Location	τ_h^a	τ_h^b
<i>Krehbiel [1981]</i>	Flash 47	Florida	2.2	3.0
...	Flash 47 (second stroke)	Florida	1.5	3.0
...	Flash 57	Florida	1.5	2.0
...	Flash 60	Florida	18	24
<i>Rust et al. [1981]</i>	Figure 3 0010:07 UTC	Oklahoma	4	10
...	Figure 6 0113:33 UTC	Oklahoma	90	140
<i>Rust [1986]</i>	Figure 3.2 0315:37.27 UTC	Oklahoma	32	45
<i>Kawasaki and Mazur [1992]</i>	Figure 3	Japan	1.5	2.0
<i>Brook (personal communication, 1994)</i>	2127:29 UTC	Oklahoma	5	11
...	2129:03 UTC	Oklahoma	6	10
...	2130:20 UTC	Oklahoma	55	65
<i>Mitchell [1997]</i>	0450:29.255 UTC	Central U.S.	2.4	3.5
...	0452:54.243 UTC	Central U.S.	2.1	3.0
...	0541:02:319 UTC	Central U.S.	1.1	3.0
...	0546:21.494 UTC	Central U.S.	1.8	2.7
...	0616:25.471 UTC	Central U.S.	1.2	1.7
...	0622:05.037 UTC	Central U.S.	1.2	1.7

^atime to transfer half the total charge (ms).

^beffective *e*-folding time for charge transfer (ms).

fact, the existence of distinct elve events in which sprites are absent raises this interest further. Conventional air breakdown is just achieved by a moment change of $Q dS = 400$ C-km in the conductivity "ledge" region (85–90 km) in Figure 3 where elves are observed [Boeck *et al.*, 1992, S. B. Mende *et al.*, unpublished manuscript, 1996]. However, the relaxation times here are submillisecond [Hale, 1984], and the time constants associated with the charge transfer that we measured (and which are included with other determinations in Table 1) are milliseconds or more. The e -folding times for the luminosity of elve-associated positive ground flashes observed from space [Mitchell, 1997] are also in the millisecond range. These observations taken together make it unlikely that conventional air breakdown is the mechanism for elves. Runaway breakdown is theoretically allowed for moment changes typical for elves but not at altitudes where elves are observed.

The largest moment changes we have observed are associated with the positive ground flashes that simultaneously produce sprites and Q bursts (i.e., red current spectra) in the Earth-ionosphere cavity. The moment changes for sprite events in Figure 7 are 5–50 times larger than those for ordinary negative ground flashes. For a moment change of $Q dS = 1000$ C-km, deposited in a time of 5 ms typical of the observed time constants (Table 1), the sprite could initiate anywhere in the altitude range 50–75 km by the electron runaway mechanism. This is the range where sprites do, in fact, initiate [Fukunishi *et al.*, 1997; Watanabe, 1999, and M. Stanley, personal communication, April 1999]. To have a sprite initiate by conventional air breakdown at 60 km, as envisioned by Wilson [1925], a moment change of about $Q dS = 3500$ C-km would be required. This value is substantially larger than all values documented in this paper. The extraordinarily large charge transfers of thousands of coulombs speculated on by Marshall *et al.* [1996] on the basis of electric field measurements within MCSs were not observed routinely in this study. Only three charge moments (among 212 total observations) from Burke and Jones [1996] exceed the value of 3500 C-km. These results support the notion that runaway breakdown is a more likely mechanism for sprites than conventional air breakdown is. The inferred mechanism is consistent with a report linking a positive ground flash and a burst of gamma rays overhead in space [Inan *et al.*, 1996a].

The conclusion drawn here concerning the inadequacy of conventional dielectric breakdown as a general explanation for sprites is contrary to Wilson's [1925] initial speculation but identical to the conclusion drawn recently by Marshall *et al.* [1995] for the initiation of lightning in thunderclouds. In the few cases for which the charge moment is sufficiently large for conventional air breakdown, one wonders why runaway breakdown would not occur first. Finally, we note in Figure 15 that as the charge moment increases to $Q dS = 10,000$ C-km, a value some four orders of magnitude larger than the smallest values considered for intracloud lightning flashes, the dielectric strength of the troposphere clearly begins to limit the maximum value.

5.5. Differences in the Morphology of Positive Ground Flashes Producing Sprites and Elves

Distinct differences in ELF radiation from positive ground flashes associated with elves and with sprites have been identified in this study. This distinction is probably most pronounced in the lower (i.e., Schumann resonance) end of the ELF band, as slow tails are observed with both elves and sprites (M. Brook and M. Stanley, personal communication, 1997). The differences in the lower ELF band mirror characteristics of the optical phenomena. Elves are relatively brief (less than one video frame), the associated NLDN return stroke currents are among the largest recorded, and the ELF spectra are white or slightly pink. Sprites are of long duration (several video frames [Lyons, 1996b]), the NLDN return stroke currents tend to be smaller (though still large in comparison with the majority of ground flashes of either polarity), and the ELF spectra are red and therefore in greater conformity with classical Q bursts. These documented differences warrant some speculation about the differences in morphology and current history for the positive ground flashes, which have not yet been documented for specific sprite and elve events (for most sprite and elve sightings from Yucca Ridge, the storms are too distant to allow direct observations of the subcloud lightning).

On the face of it, these differences would suggest highly charged leader channels for elve lightning, without extensive branching aloft, in light of the short-duration continuing currents (e.g., Figure 5h). For sprite lightning an extensive dendritic structure is required to account for the long continuing current [Heckman and Williams, 1989], though the charge on the leader channel would appear to be less, on average, than that for elves. The inference for an extensive discharge structure aloft is consistent with the broad diffuse light emanating from the MCS beneath the red sprite ("Big Red") documented from an aircraft by the University of Alaska [Osborne, 1994].

One possible electrostatic explanation for these differences is illustrated in Figure 16. In MCSs producing elves and sprites the charge regions appear to be more sheet-like than point-like [Krehbiel, 1981; Stolzenburg *et al.*, 1994;

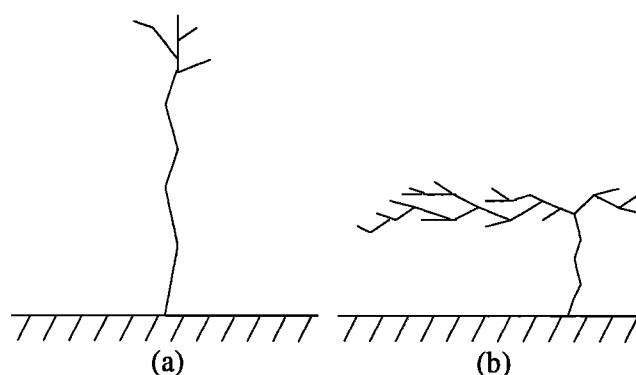


Figure 16. Speculative structures (post return stroke channel illumination) for positive ground flashes causal to (a) elves and (b) sprites.

Marshall et al., 1996]. For charge sheets with fixed charge per unit area, the potential of the sheet is linear with the sheet's altitude. A positive leader that descends from a positive sheet at high altitude (Figure 16a) may therefore carry more cloud potential toward ground than the same sheet at intermediate altitude does (Figure 16b) and consequently charge its conductive channel more strongly than the case for the lower charge sheet [*Heckman and Williams*, 1989]. The mean return stroke current associated with the elves is roughly twice that for the sprites on the basis of the results in Figure 13. In contrast, the return stroke extension may pervade the lower layer (Figure 16b) more easily to produce long continuing current than it does in the upper sheet, owing to the larger potential drop in the longer vertical channel in the latter case. The discharge structure in Figure 16b is akin to the forms observed in laboratory experiments in which the space charge was also sheet-like [*Williams et al.*, 1985].

Elve events are notably less common than sprite events. This is illustrated in the histograms in Figure 13 and by the event counts for the July 24, 1996, storm reported earlier in section 3.3. These event observations would suggest that positive ground flashes from a lower charge reservoir are more common lightning events [*Williams*, 1998].

5.6. The Issue of Sprite Ionization

The observation that the dominant red optical emission from sprites is associated with neutral nitrogen [*Mende et al.*, 1995; *Hampton et al.*, 1996] has led to suggestions that sprites are not ionized [*Hampton et al.*, 1996]. *Armstrong et al.* [1998] have presented evidence for the appearance of blue emission at 427.8 nm associated with ionized nitrogen that appears very early in the sprite breakdown process. Furthermore, *Dowden et al.* [1996] have interpreted the scattering of VLF radiation from sprites as requiring an ionized medium. The comparisons here between the charge moments and the electric fields in the Wilson diagram (Figure 15) are clearly relevant to the unresolved issue of sprite ionization.

Conventional dielectric breakdown [*Wilson*, 1925], runaway electron breakdown [*Gurevich et al.*, 1992; *Bell et al.*, 1995], and electron heating [*Pasko et al.*, 1995] have all been invoked in theoretical treatments of the origin of sprites. The comparison of measured moment changes with the Wilson diagram indicates that conventional dielectric breakdown, with its attendant ionization, is unlikely for the majority of sprite events. The favored interpretation of the present observations, however, is electron runaway breakdown. Theoretical simulations of this process [*Taranenko and Roussel-Dupré*, 1996] do predict the presence of ionized nitrogen and therefore a source of surplus electrons to enhance the sprite conductivity.

5.7. Interpretation of Source Charge Moment and the Role of Sprites in ELF Radiation

In interpreting the Schumann resonance signals emanating from sprite and elve events, we have adhered to the assumption that the charge moment $Q dS$ in the normal mode

equations (equations (3) and (4)) is dominated by the parent lightning in the troposphere, with a negligible contribution from the mesospheric phenomena. The largest measured moment changes in Figures 7–9 are of order hundreds of coulomb-kilometers and are clearly an order of magnitude larger than values in ordinary thunderclouds. This fact clearly contributed to early skepticism that Q bursts had origins in thunderclouds [*Ogawa et al.*, 1967]. At that time, however, little information was available about either the extraordinary nature of positive ground flashes or the extensive charge storage in mesoscale convective systems, which were not even named until the 1980s [*Zipser*, 1982].

Despite the recognition of the more recent information, speculation continues on the role of the sprites themselves in contributing to ELF radiation. This speculation extends as far as identifying the moment length dS with the sprite altitude (~ 60 km), consistent with *Wilson* [1956], who suggested that the discharge extended from the cloud top to the ionosphere. Other speculation includes the claim that the ELF radiation from the sprite volume itself may dominate the radiation from the parent lightning [*Inan et al.*, 1997; *Cummer et al.*, 1998].

Some simple calculations are in order to examine these suggestions. In the present interpretation of results, a measured moment change of $Q dS = 500$ C-km invokes a positive charge transfer of 100 C from a $dS = 5$ km height, the altitude range where extensive "spider" lightning is observed [*Boccippio et al.*, 1995; *Marshall et al.*, 1996; *Williams*, 1998; *Mazur et al.*, 1998]. Given present knowledge of the electrical structure of the stratiform region of mesoscale convective systems [*Krehbiel*, 1981; *Marshall et al.*, 1996], a charge transfer of 100 C is quite reasonable. If dS were identified instead with the sprite altitude and were consequently increased by an order of magnitude, then Q would be proportionally reduced to 10 C. Such a small charge transfer (of the order of the value in a negative ground flash in an ordinary thundercloud) to account for the ELF observations is inconsistent with available information on the charge in MCSs [*Krehbiel*, 1981; *Marshall et al.*, 1996] and is implausible.

In evaluating the ELF radiation from the sprite body itself, consideration is given again to a simple electrostatics calculation. Following the indirect evidence from the Wilson diagram for sprite ionization by a runaway breakdown process on a timescale short in comparison with the local relaxation time, the sprite is modeled as a conductive sphere of radius a at height z above the conductive Earth. The electric field E , which causes the ionization, and the spherical conductivity perturbation are given by (1) for a point dipole. If the dipole field is assumed uniform in the vicinity of the sprite, the induced dipole moment p' is analytically described by *Stratton* [1941]:

$$p' = 4\pi\epsilon_0 E a^3 [C \cdot m]. \quad (21)$$

According to electromagnetic theory from which the normal mode equations were derived [*Wait*, 1996], the ELF radiation amplitude is proportional to the charge moment p of the lightning source (equation (1)), [see also *Sentman*, 1996]. The ratio of the radiation amplitude from the sprite to that

from the parent lightning is simply the ratio of the respective moment changes:

$$\frac{p'}{p} = 2 \frac{a^3}{z^3}. \quad (22)$$

This ratio depends only on the size of the sprite and its altitude. For typical values for these quantities, $a = 20$ km and $z = 60$ km,

$$\frac{p'}{p} = \frac{2}{27}. \quad (23)$$

This comparison casts some doubt on the assertion [Inan *et al.*, 1997; Cummer *et al.*, 1998] that the radiation from the sprite will dominate that of the parent lightning unless the conductive sprite volume is substantially greater than the luminous region in the LLTV observations. In the work of Cummer *et al.* [1998] all of the observed ELF signature is attributed to the sprite, and none is attributed to the parent lightning.

According to the physical mechanism for mesospheric breakdown discussed here, sprites are more likely to occur if the lightning charge is transferred in a time less than the relaxation time aloft. The information on this quantity in Figure 3 suggests a strong day-night difference at altitudes where sprites are observed to initiate at night. At 60 km altitude the nighttime relaxation time is an order of magnitude greater than that during the day. For a fixed transfer of charge, sprites are therefore expected to be more likely at night than during the day. If ELF radiation is dominated by the sprite, we can expect stronger ELF radiation, on average, from positive ground flashes at night than during the day. Unfortunately, all of the transient events studied in detail in this paper occurred at night, a situation dictated by mesoscale meteorology. A search for a change in the detection efficiency (number of ELF events recorded in comparison with the number of positive ground flashes recorded by the NLDN for a fixed ELF recording threshold) of ELF transients for a month's worth of data showed no discernible change across the local sunset time.

Given the evidence here for a dominance of ELF radiation from the parent ground flash, experimental efforts to quantify the charge transfer within the sprite itself with ELF methods will be thwarted by the near simultaneous lightning "noise" which is the main "signal" in this paper.

5.8. The Issue of Sprite Brightness and Its Dependence on the Lightning Charge Moment

The purpose of the sprite brightness measurements and their comparison with the ELF observations was twofold: (1) to ascertain that the full dynamic range of sprite brightness, obtained with state-of-the-art optical equipment, was examined with Schumann resonance methods and (2) to test certain theoretical predictions [Pasko *et al.*, 1995; Bell *et al.*, 1995] for the dependence of sprite optical intensity on the charge transfer by the parent lightning. The first goal was achieved at the high end of the sprite brightness scale, but at the low end no events with "very faint" characterization (~ 2000 counts) were processable for charge moment with the ELF methods available. The pursuit of the second goal

led to examination of theoretical predictions for the dependence of sprite optical intensity on charge transfer in the parent lightning. The predictions for both a quasi-electrostatic heating mechanism [Pasko *et al.*, 1995] and an electron run-away mechanism [Bell *et al.*, 1995] were examined. In the former study, a doubling of lightning charge moment causes more than a hundredfold increase in optical intensity. In the latter study, the dependence is still stronger: a six decade increase in optical intensity for a 50% increase in charge moment. These dependences are inconsistent with the observations in Figure 12 which suggest an approximate linear relationship between charge moment and sprite brightness. The reasons for this discrepancy are not well understood at present.

5.9. The Issue of Polarity Asymmetry for the Parent Lightning

The predictions for electrical breakdown of the upper atmosphere outlined by Wilson [1925] and summarized in Figure 15 are entirely independent of the polarity of the charge moments. This situation emphasizes the polarity asymmetry clearly evident in sprite phenomena: positive ground flashes are almost exclusively favored as sources for these events [Bocippio *et al.*, 1995; Lyons, 1996b]. Every event presented in Figure 13 is associated with a positive ground flash independently verified by the National Lightning Detection Network. Does this pronounced asymmetry have its origin in meteorology or in discharge physics?

Numerous results support the idea that the peak currents, durations, and total charge transfers associated with positive ground flashes exceed those from negative flashes. Meteorological differences are very likely responsible to a considerable extent. Negative lightning accompanies ordinary thunderstorms with dominant lower negative charge. Positive lightning is more prevalent in the stratiform precipitation regions of mesoscale convective systems with dominant lower positive charge which is more laterally extensive [Marshall *et al.*, 1996; Williams, 1998]. Charge reservoirs in different meteorological regimes have been reviewed by Williams [1995, 1998]. Despite the 10 to 1 prevalence of negative ground flashes over positive ground flashes documented by numerous lightning detection networks over the last decade, the positive polarity is more prevalent in global maps based on Schumann resonance methods (see [Burke and Jones, 1995, 1996], [Yamamoto and Ogawa, 1996], and this study). When negative flashes with extraordinarily large (>75 kA) peak current (according to the NLDN) were examined in our Rhode Island ELF data archive, only a small fraction exceeded our recording threshold. We interpret this result to mean that despite the large peak current, the durations for negative flashes tend to be small, and hence the total moment change is insufficient to produce strong ELF radiation.

This is not to say, however, that there are no negative ground flashes with sufficient charge moments to trigger breakdown thresholds in Figure 15. Negative events with moment changes of thousands of coulomb-kilometers are detected by the Rhode Island system and in other ELF measurements [Burke and Jones, 1996]. Given the time con-

stants documented in the latter study, some of these large negative events are legitimately Q bursts in *Ogawa et al.'s* [1967] original sense. We have not yet pinpointed the meteorological conditions (or the diurnal variation) in which these events occur, but they do exist [see also *Lyons et al.*, 1998]. This result indicates that meteorological conditions are not exclusively responsible for the positive bias in the results, and it suggests that discharge physics is playing a role.

The measured moment changes for the sprite events have already indicated that runaway breakdown is a candidate physical mechanism for sprites. This runaway process is necessarily vertical and takes place in a medium with a vertical density gradient. The predicted electron avalanche length for this process [*Symbalisy et al.*, 1998] is roughly equal to the density scale height (~ 7 km) at ~ 50 km and is progressively larger than the density scale height at greater altitudes. At a height of 70 km, for example, the predicted avalanche length is 50 km. If the avalanche length were small in comparison to the scale height, we would not expect polarity asymmetry. Indeed, for conventional dielectric breakdown of air, the relevant scale is the electron mean free path which is 10 μm at sea level, 20 mm at 50 km, and 30 cm at 70 km, all substantially smaller than the density scale height. The need for electrons to runaway upward into the lower density upper atmosphere may therefore constitute the fundamental requirement for ground flashes of positive polarity.

5.10. The Issue of Time Sequence: Positive Return Stroke and Sprite

According to the mechanism invoked here and elsewhere [*Boccippio et al.*, 1995; *Pasko et al.*, 1995; *Bell et al.*, 1995], the charge transferred by the return stroke and continuing current following the positive return stroke is responsible for electrostatically stressing the mesosphere and creating the sprite. In continuing currents studied in ordinary thunderclouds, the continuing current immediately follows the return stroke in the same channel to ground with a monotonic decay [*Brook et al.*, 1962], hence the simplifying assumption in the present study of a current of exponential form. The need for the bulk of the charge transfer to occur in a time of the order of the local ionospheric electrostatic relaxation time or less has been emphasized. In this scenario the sprite should occur within a local relaxation time at the altitude of sprite initiation, consistent with the earliest report by *Fukunishi et al.* [1996].

The time lags between the NLDN return strokes and the paired elves and sprites for the July 24, 1996, storm were presented in Figure 11. At the timescale resolved by the video observations the lag for the elves is very short, consistent with the idea that the elves are produced by the return stroke radiation field (EMP) [*Inan et al.*, 1996b], which is not resolved by the bandwidth available in the present Schumann resonance observations. The predicted speed-of-light time delay from the ground end of the return stroke channel to typical elve altitude (90 km) is 0.3 ms, which is essentially zero on the timescale in Figure 11b. The short observed lag does not rule out an electrostatic mechanism for the elves

by itself, however. In either case for the elves the near-zero lag provides confidence that the timing for the video camera observations and the NLDN observations are accurate at the millisecond timescale.

In contrast with Figure 11b, the lag times for the sprites show a strong positive tendency. The most probable lag is in the range of 1–8 ms (with nearly one third of all analyzed events in this range), consistent with the idea that the charge transfer following the positive return stroke, in a time comparable to the local electrostatic relaxation time (Figure 3), is causing dielectric breakdown (of some kind) in the mesosphere forming the sprite. Over half of all events lie within the 1–16 ms window following the return stroke. Not all the lags documented in Figure 11a are consistent with this simple electrostatic picture, however. A minority fraction of events (11%) show lags exceeding 70 ms, and a smaller fraction of events ($\sim 6\%$) show appreciable negative lags. The finding of large positive lags in a similar analysis of sprites by *Bell et al.* [1998] led the latter investigators to question the positive ground flash and its subsequent continuing current to ground as a causal agent. Alternative explanations for the outliers in Figure 11a seem more likely:

1. The pairing of events may be incorrect. A more rigorous analysis would consider the bearing to the sprite and its comparison with the paired ground flash location.
2. The NLDN occasionally misses strokes of positive ground flashes. The received waveform for these large and energetic discharges may be quite complicated and fail to satisfy the NLDN criteria for positive ground flashes.
3. The return stroke-continuing current evolution may not be monotonic and may depart from the simple exponential behavior assumed in section 2.6.3. Both *Mitchell* [1997] and *Armstrong et al.* [1998] have provided evidence in optical observations for a distinct secondary maximum in the continuing current for sprite-associated positive ground flashes that may be delayed from the return stroke by some tens of milliseconds. The sprite could well be initiated by the charge transfer in the delayed continuing current. The physical explanation for the delay may be related to the laterally extensive charge reservoir aloft from which the positive charge is evidently drawn [*Marshall et al.*, 1996; *Williams*, 1998] in the long continuing currents.

5.11. The Issue of Model Accuracy

Conclusions are drawn in this paper about physical mechanisms for sprite formation on the basis of inferred moment changes in parent positive ground flashes. The numbers for moment change rest on calibrated field measurements and on a model for the Earth-ionosphere cavity. The model represented by (3) and (4) pertains to a uniform cavity which is an approximation to the real cavity. The implications of this difference deserve some discussion.

Madden and Thompson [1965], *Bliokh et al.* [1980], *Sentman and Fraser* [1991], and *Burke and Jones* [1992] have all called attention to departures from spherical symmetry in the Earth-ionosphere cavity in the Schumann resonance frequency range based on both theory and experiment. These departures lead to differences in the measured fields which

are of the order of tens of percent from those predicted for a uniform cavity. While such variations are large in comparison to the absolute uncertainty of the field measurements reported here and by *Heckman et al.* [1998], they do not lead to grave distortions at the continental scale in global maps of transient locations. This claim pertains both to earlier work [*Kemp*, 1971; *Burke and Jones*, 1992; *Yamamoto and Ogawa*, 1996] and to the present capabilities for global mapping from the Rhode Island station shown in Figure 17.

In analyzing events we rely on single-station measurements to locate events. The availability of NLDN identification of positive ground flashes for North America has enabled comparisons with the single-station ELF locations. These comparisons have shown that we systematically overestimate the distance between the source and the receiver by ~ 100 km, and our results exhibit a bearing error that varies sinusoidally with direction. This bearing error is accounted for in the analyses [*Huang*, 1998]. The range error is less well understood (it may be caused by errors in the wave impedance theory) and remains uncorrected.

The accuracy of the inferred charge moments is the major issue here. Perhaps the most convincing accuracy test (while presently unavailable) would be a simultaneous measurement and comparison of charge moment by the conventional electrostatic method [*Jacobson and Krider*, 1976; *Krehbiel et al.*, 1979] and the electromagnetic method discussed here. Owing to the extended nature of the charge reservoir in sprite-producing MCSs [*Bocippio et al.*, 1995; *Lyons*, 1996b; *Williams*, 1998], the implementation of the conventional electrostatic method meets with some difficulty. If the field change measurements are too close to the MCS, the point source assumption is invalid, and if the measurements are too far (i.e., comparable to one ionospheric height), the conventional electrostatic formulae are invalid [*Pumplin*, 1969].

An alternative approach toward gauging the accuracy of the moment change estimates is to consider the uniform cavity interpretation of ELF fields from simulated point sources in a theoretical model for the cavity that includes recognized asymmetry. Such an approach (*V. Mushtak*, personal communication, 1998) suggests that the inferred moment changes may be in error by some tens of percent. Errors of this magnitude do not invalidate the main conclusion that

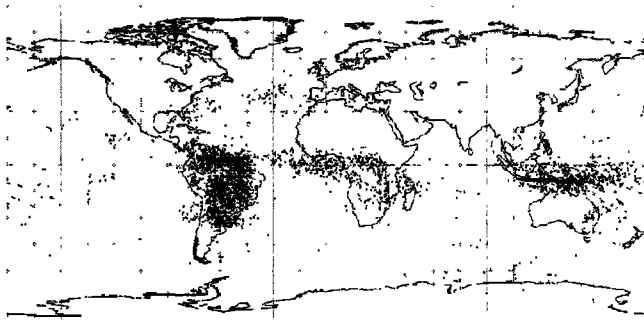


Figure 17. Global map for January 1996 based on measurements in West Greenwich, Rhode Island.

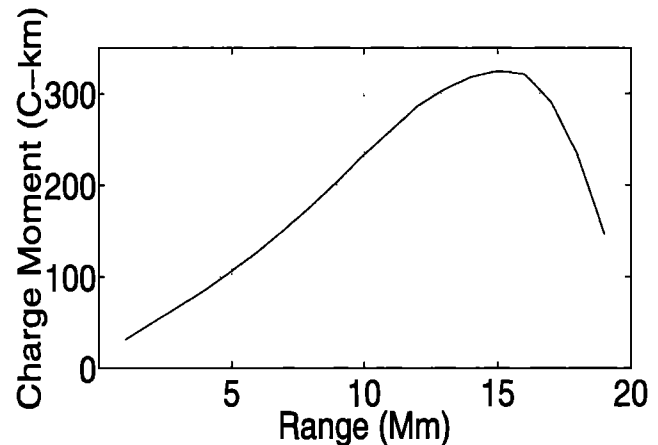


Figure 18. Detection threshold for the magnetic trigger within the practical range interval (1–19 Mm) for event detection. A bandwidth of 120 Hz is assumed.

the observed moment changes for sprites are generally insufficient to provoke conventional air breakdown in the mesosphere as was originally suggested by *Wilson* [1925].

5.12. The Issue of Global Detection of Sprites and Elves

The Schumann resonance methods are inherently global. The analyses presented here are largely confined to North American events because of their optical verification and characterization from Yucca Ridge. There is little question that energetic positive ground flashes in other parts of the world are also producing sprites and elves and simultaneously “ringing” the Earth-ionosphere cavity. The detectability of such events from the Rhode Island station is considered here.

Figure 18 shows calculations for the critical charge moment of an impulsive lightning source needed to trigger the Rhode Island system (with its present $11.6 \mu\text{A/m}$ trigger threshold on H_ϕ) over the full range of practical source-receiver distances (1–19 Mm). These predictions are based on the normal mode equation for the magnetic field (equation (4)). Experimental results in Figure 7, based on measurements on the July 24, 1996, storm at a distance of ~ 2 Mm, suggest that the threshold charge moment for “very faint” sprites is about $Q dS = 300$ C-km. (For elves the charge moment is not the relevant threshold quantity if the radiation field rather than the electrostatics field is their cause.) Comparison with the plot in Figure 18 indicates that a 300 C-km event would trigger the Rhode Island system regardless of its location, except events in the distance range 12–16 Mm. Given the rather high threshold setting for present recording, this comparison verifies the sensitivity to sprite events on a global basis with single-station Schumann resonance methods. At short distances the sensitivity to moment change with our 120 Hz bandwidth (exceptionally wide compared with most other Schumann resonance measurements) is an order of magnitude greater than the presumed sprite threshold, and so numerous transient events are detected. For this reason the Americas show many more

events than more distant Africa and Asia do in global maps from Rhode Island (Figure 17).

5.13. The Issue of System Bandwidth and Exponential Time Constants

The time constants τ that we measure using the exponential fit method described in section 2.6.3 result in average values of ~ 5 ms for sprites, which compares favorably with the electrostatic relaxation time in Figure 3 for an altitude of 60 km. As Table 2 shows, there is significant variation in time constants measured by *Burke and Jones* [1996], *Bell et al.* [1998], and this study. *Burke and Jones* measured very long time constants, which are too long according to Figure 3 to allow sprites (although we do not know if any of the events in that study produced sprites). By contrast, the current moments from *Bell et al.* have time constants that are significantly less than a millisecond. Perhaps not by coincidence, the measurements with the smallest bandwidth had the highest numbers for the time constants. A possible explanation comes from *Cummer et al.* [1998], where the waveforms often show a two-component (at least) current moment, with an initial, short-duration decaying current followed by a second peak that decays more slowly. By not being able to discern the higher frequencies in the Stanford measurements, neither *Burke and Jones* nor the present measurements are able to resolve the initial faster component, and therefore the derived time constants are longer. Conversely, the weak response at low frequencies in the bandwidth of *Cummer et al.* (they do not detect the first two modes of the Schumann resonances) might cause them to derive much shorter-duration waveforms. In future measurements it is strongly recommended that bandwidths from 3 Hz to many kilohertz be used to resolve such discrepancies. In reality, the lightning current is not a single time constant phenomenon but rather shows decay on many different timescales.

6. Conclusions

This study extends the documentation of a clear connection between upper atmospheric optical phenomena, elves and sprites, with the most energetic lightning flashes of positive polarity. The latter circumstance guarantees the strongest signals in the Earth-ionosphere cavity and the applicability of Schumann resonance methods in analyzing the source properties of these events. The basic predictive framework suggested by *Wilson* [1925] has been validated with electromagnetically measured charge moments. The

values for these charge moments and the nearly exclusive association of sprites with ground flashes of positive polarity are both consistent with an electron runaway mechanism for dielectric breakdown in the mesosphere. Considerations of the electrostatic relaxation time and the lag times from the positive return strokes to the time of peak sprite brightness suggest that the majority of lightning charge transfer takes place in a few milliseconds. The sustained current flow for longer times is enabled by the laterally extensive positive charge reservoirs in the MCS [*Williams*, 1998; *Mazur et al.*, 1998]. The long continuing current is probably responsible for both the red nature of Q bursts and for the sustained sprite luminosity (at lower levels of intensity) in the LLTV observations.

In contrast with sprite events, elve events exhibit nearly white ELF spectra in a band pass which is too narrow to analyze the return stroke radiation field. The NLDN observations of large peak currents for elve events do, however, substantiate the EMP mechanism suggested in earlier work [*Inan et al.*, 1996b; *Armstrong et al.*, 1998]. Further Schumann resonance analysis of source properties for positive ground flashes beneath the daytime and nighttime ionospheres is needed to assess the existence of daytime sprites. Improved documentation of x-ray emission from MCSs is needed to verify the runaway electron mechanism for sprite initiation.

Note added in proof: *M. Stanley* (personal communication, 1999) has recently reported sprite initiation heights systematically higher than those reported by *Fukunishi et al.* [1997] and *Watanabe* [1999], results on which the interpretations in this paper were based. A higher sprite initiation altitude makes possible sprite initiation by conventional air breakdown for a larger number of observed charge moments. Further studies are needed of charge moments and initiation altitudes for the same event to clarify this issue.

Acknowledgments. Discussions and exchanges with the following individuals contributed substantially to this research: *R. Armstrong*, *T. Bell*, *D. Boccippio*, *B. Boeck*, *M. Brook*, *L. Carey*, *K. Cummins*, *E. Dewan*, *D. Dowden*, *D. Free*, *H. Fukunishi*, *M. Fullekrug*, *L. Hale*, *M. Hayakawa*, *U. Inan*, *M. Ishii*, *R. Jayaratne*, *L. Jeong*, *D. Jones*, *P. Krehbiel*, *D. Latham*, *T. Madden*, *V. Mazur*, *E. Mitchell*, *C. B. Moore*, *V. Mushtak*, *A. Nickolaenko*, *T. Ogawa*, *V. Pasko*, *C. Polk*, *C. Price*, *S. Reising*, *K. Rothkin*, *R. Roussel-Dupré*, *G. Satori*, *A. Seimon*, *D. Sentman*, *Y. Takahashi*, *H. Torres*, *J. Wait*, *Y. Yair*, and *V. Yukhimuk*. We thank *T. Mitchell* at the Alton Jones Campus of the University of Rhode Island for site access and *M. Stewart* of the NASA MSFC for electronic equipment. The Grainger Foundation (*David Grainger*) has provided generous support for recording equipment at the RI field station. This research has been supported by Physical Meteorology (*R. Rogers* and *R. Taylor*) and Climate Dynamics (*J. Fein*) at the National Science Foundation (ATM 963 3766), by Phillips Laboratory (*L. Jeong*) on grant (F1 9628-96-C-0087), and by an MIT subcontract (SC-0161-97-0) with the Mission Research Corporation (*R. Armstrong*). *M. J. Taylor* acknowledges support from AFPL on contract F193628-93-C-0165.

References

Armstrong, *R. A.*, *J. A. Shortor*, *M. J. Taylor*, *D. M. Suszcynsky*, *W. A. Lyons*, and *L. S. Jeong*, Photometric measurements in the SPRITES '95 & '96 campaigns: Nitrogen second positive

Table 2. Comparison of Continuing Current Time Constants for Positive Ground Flashes Observed with Different Bandwidths

Investigator	Bandwidth, Hz	τ_{avg} , ms
<i>Bell et al.</i> [1998]	15–24,000	<1
<i>Burke and Jones</i> [1996]	5–45	32
This study	3–120	3–6

- (399.8 nm) and first negative (427.8 nm) emission, *J. Atmos. Sol. Terr. Phys.*, **60**, 787, 1998.
- Bell, T. F., V. P. Pasko, and U. S. Inan, Runaway electrons as a source of red sprites in the mesosphere, *Geophys. Res. Lett.*, **22**, 2127, 1995.
- Bell, T. F., S. C. Reising, and U. S. Inan, Intense continuing currents following positive cloud-to-ground lightning associated with red sprites, *Geophys. Res. Lett.*, **25**, 1285, 1998.
- Bliokh, P. V., A. P. Nickoanenko, and Y. V. Filippov, *Schumann Resonances in the Earth-Ionosphere Cavity*, Peter Peregrinus, London, 1980.
- Boccippio, D. J., E. R. Williams, S. J. Heckman, W. A. Lyons, I. T. Baker, and R. Boldi, Sprites, ELF transients, and positive ground strokes, *Science*, **269**, 1088, 1995.
- Boccippio, D. J., C. Wong, E. Williams, R. Boldi, H. Christian, and S. Goodman, Global validation of single-station Schumann resonance lightning location, *J. Atmos. Sol. Terr. Phys.*, **60**, 701, 1998.
- Boeck, W. L., O. H. Vaughan, R. Blakeslee, B. Vonnegut, and M. Brook, Lightning induced brightening in the airglow layer, *Geophys. Res. Lett.*, **19**, 99, 1992.
- Brook, M., N. Kitagawa, and E. J. Workman, Quantitative study of strokes and continuing currents in lightning discharges to ground, *J. Geophys. Res.*, **67**, 649, 1962.
- Burke, C. P., and D. L. Jones, An experimental investigation of ELF attenuation rates in the Earth-ionosphere duct, *J. Atmos. Terr. Phys.*, **54**, 243, 1992.
- Burke, C. P., and D. L. Jones, Global radiolocation in the lower ELF frequency band, *J. Geophys. Res.*, **100**, 26,263, 1995.
- Burke, C. P., and D. L. Jones, On the polarity and continuing currents in unusually large lightning flashes deduced from ELF events, *J. Atmos. Terr. Phys.*, **58**, 531, 1996.
- Cummer, S. A., and U. S. Inan, Measurement of charge transfer in sprite-producing lightning using ELF radio atmospheric, *Geophys. Res. Lett.*, **24**, 1731, 1997.
- Cummer, S. A., U. S. Inan, T. F. Bell, and C. P. Barrington-Leigh, ELF radiation produced by electrical currents in sprites, *Geophys. Res. Lett.*, **25**, 1281, 1998.
- Dowden, R. L., J. Brundell, C. Rodger, O. Molchanov, W. Lyons, and T. Nelson, The scattering of red sprites determined by VLF scattering, *IEEE Trans. Antennas Propag.*, **38**, 7, 1996.
- Franz, R. C., R. J. Nemsek, and J. R. Winkler, Television image of a large upward electrical discharge above a thunderstorm system, *Science*, **249**, 48, 1990.
- Fukunishi, H., Y. Takahashi, M. Kubota, K. Sakanoi, U. S. Inan, and W. A. Lyons, Elves: Lightning-induced transient luminous events in the lower ionosphere, *Geophys. Res. Lett.*, **23**, 2157, 1996.
- Fukunishi, H., Y. Takahashi, M. Fujito, and Y. Watanabe, Fast imaging of elves and sprites using a framing/streak camera and a multi-anode array photometer, paper presented at Int. Union of Geod. and Geophys., Uppsala, Sweden, 1997.
- Garcia, F. J., M. J. Taylor, and M. C. Kelley, Two-dimensional spectral analysis of mesospheric airglow image data, *Appl. Opt.*, **36**, 7374, 1997.
- Gurevich, A. V., G. M. Milikh, and R. Roussel-Dupré, Runaway electron mechanism of air breakdown and preconditioning during a thunderstorm, *Phys. Lett. A*, **165**, 463, 1992.
- Hale, L. C., Middle atmosphere electrical structure, dynamics, and coupling, *Adv. Space Res.*, **4**, 175, 1984.
- Hampton, D. L., M. J. Heavner, E. M. Wescott, and D. D. Sentman, Optical characteristics of sprites, *Geophys. Res. Lett.*, **23**, 89, 1996.
- Heckman, S., and E. Williams, Corona envelopes and lightning currents, *J. Geophys. Res.*, **94**, 13,287, 1989.
- Heckman, S. J., E. Williams, and R. Boldi, Total global lightning inferred from Schumann resonance measurements, *J. Geophys. Res.*, **103**, 31,775, 1998.
- Huang, E. W., Electromagnetic transients, elves, and red sprites in the Earth-ionosphere waveguide, M.Eng. thesis, Mass. Inst. of Technol., Cambridge, 1998.
- Inan, U. S., S. C. Reising, G. J. Fishman, and J. M. Horack, On the association of terrestrial gamma-ray bursts with lightning and implications for sprites, *Geophys. Res. Lett.*, **23**, 1017, 1996a.
- Inan, U. S., W. A. Sampson, and Y. N. Taranenko, Space-time structure of optical flashes and ionization changes produced by lightning-EMP, *Geophys. Res. Lett.*, **23**, 133, 1996b.
- Inan, U. S., T. F. Bell, and D. S. Lauben, ELF radiation from sprites and its effects on the upper ionosphere and the radiation belts, *Eos Trans. AGU*, **78**(46), Fall Meet. Suppl., F70, 1997.
- Ishaq, M., and D. L. Jones, Methods of obtaining radiowave propagation parameters for the Earth-ionosphere duct at ELF, *Electron. Lett.*, **13**, 254, 1977.
- Jacobson, E. A., and E. P. Krider, Electrostatic field changes produced by Florida lightning, *J. Atmos. Sci.*, **33**, 103, 1976.
- Jones, D. L., Schumann resonances and ELF propagation for inhomogeneous isotropic ionospheric profiles, *J. Atmos. Terr. Phys.*, **29**, 1037, 1967.
- Jones, D. L., and D. T. Kemp, The nature and average magnitude of the sources of transient excitation of the Schumann resonances, *J. Atmos. Terr. Phys.*, **33**, 557, 1971.
- Kawasaki, Z. I., and V. Mazur, Common physical processes in natural and triggered lightning in winter storms in Japan, *J. Geophys. Res.*, **97**, 12,935, 1992.
- Keefe, T. J., H. Etzold, and C. Polk, Detection and processing of ELF (3–30 Hz) natural electromagnetic noise, *Tech. Rep., AFCRL-TR-73-0077*, Air Force Cambridge Res. Lab., Bedford, Mass., 1973.
- Kemp, D. T., The global radiolocation of large lightning discharges from single station observations of ELF disturbances in the Earth-ionosphere waveguide, *J. Atmos. Terr. Phys.*, **33**, 919, 1971.
- Koshak, W., Analysis of lightning field changes produced by Florida thunderstorms, *NASA Tech. Rep. TM-103539*, 152 pp., 1991.
- Krehbiel, P. R., An analysis of the electric field change produced by lightning, Ph.D. thesis, Univ. of Manchester, Manchester, England, 1981.
- Krehbiel, P. R., M. Brook, and R. A. McCrory, An analysis of the charge structure of lightning discharges to ground, *J. Geophys. Res.*, **84**, 2432, 1979.
- Krider, E. P., Electrostatic field changes and cloud electrical structure, *J. Geophys. Res.*, **94**, 13,145, 1989.
- Krider, E. P., On the peak electromagnetic fields radiated by lightning return strokes toward the middle-atmosphere, *J. Atmos. Electr.*, **14**, 17, 1994.
- Lyons, W. A., Characteristics of luminous structures in the stratosphere above thunderstorms as images by low-light video, *Geophys. Res. Lett.*, **21**, 875, 1994.
- Lyons, W. A., Sprite observations above the U. S. High Plains in relation to their parent thunderstorm systems, *J. Geophys. Res.*, **101**, 29,641, 1996a.
- Lyons, W. A., Sensor system to monitor cloud-to-stratosphere electrical discharges, *NASA Tech. Rep. 10-12113*, 225 pp., 1996b.
- Lyons, W. A., M. Uliasz, and T. E. Nelson, A climatology of large peak current cloud-to-ground lightning flashes in the contiguous United States, *Mon. Weather Rev.*, **126**, 2217, 1998.
- Mackerras, D., A comparison of discharge processes in cloud and ground lightning flashes, *J. Geophys. Res.*, **73**, 1175, 1968.
- Madden, T., and W. Thompson, Low-frequency electromagnetic oscillations of the Earth-ionosphere cavity, *Rev. Geophys.*, **3**, 211, 1965.
- Marshall, T. C., M. P. McCarthy, and W. D. Rust, Electric field magnitudes and lightning initiation in thunderstorms, *J. Geophys. Res.*, **100**, 7097, 1995.
- Marshall, T. C., M. Stolzenburg, and W. D. Rust, Electric field measurements above mesoscale convective systems, *J. Geophys. Res.*, **101**, 6979, 1996.

- Mazur, V., X.-M. Shao, and P. R. Krehbiel, "Spider" lightning in intracloud and positive cloud-to-ground flashes, *J. Geophys. Res.*, **103**, 19,811, 1998.
- Mende, S. B., R. L. Rairden, G. R. Swenson, and W. A. Lyons, Sprite spectra: N₂ first positive band identification, *Geophys. Res. Lett.*, **22**, 2633, 1995.
- Mitchell, E. A., Comparison of M46 broad-band visible data with ELF data from the SPRITES '96 campaign, *Sandia Nat. Lab. Tech. Rep. SAND, 97-2381 UC-703*, 132 pp., 1997.
- Nelson, T. E., Spatial relationships between radar reflectivity and sprite and elve producing cloud-to-ground lightning strikes, M.S. thesis, Mankato State Univ., Mankato, Minn, 1997.
- Nickolaenko, A. P., Modern aspects of Schumann resonance studies, *J. Atmos. Sol. Terr. Phys.*, **59**, 805, 1997.
- Ogawa, T., Y. Tanaka, M. Yasuhara, A. C. Fraser-Smith, and R. Gendrin, Worldwide simultaneity of occurrence of a Q-type ELF burst in the Schumann resonance frequency range, *J. Geomagn. Geoelectr.*, **19**, 377, 1967.
- Osborne, D., Red Sprites and Blue Jets [video tape], Geophys. Inst., Univ. of Alaska, Fairbanks, July 1994.
- Pasko, V. P., U. S. Inan, Y. N. Taranencko, and T. F. Bell, Heating, ionization and upward discharges in the mesosphere due to intense quasi-electrostatic thundercloud fields, *Geophys. Res. Lett.*, **22**, 365, 1995.
- Pierce, E. T., Atmospherics and radio noise, in *Lightning*, edited by R. H. Golde, vol. 1, pp. 358–359, Academic, San Diego, Calif., 1977.
- Polk, C., *Handbook of Atmospheric*, CRC Press, Boca Raton, Fla., 1982.
- Pumplin, J., Application of Sommerfeld-Watson transformation to an electrostatics problem, *Am. J. Phys.*, **37**, 737, 1969.
- Reising, S. C., U. S. Inan, T. F. Bell, and W. A. Lyons, Evidence for continuing current in sprite-producing cloud-to-ground lightning, *Geophys. Res. Lett.*, **23**, 3639, 1996.
- Roussel-Dupré, R., and A. V. Gurevich, On runaway breakdown and upward propagating discharges, *J. Geophys. Res.*, **101**, 2297, 1996.
- Rust, W. D., Positive cloud-to-ground lightning, in *The Earth's Electrical Environment*, National Academy Press, 1986.
- Rust, W. D., D. R. MacGorman, and R. T. Arnold, Positive cloud-to-ground lightning flashes in severe storms, *Geophys. Res. Lett.*, **8**, 791, 1981.
- Sentman, D. D., Schumann resonance spectra in a two-scale-height earth-ionosphere cavity, *J. Geophys. Res.*, **101**, 7097, 1996.
- Sentman, D. D., and B. J. Fraser, Simultaneous observations of Schumann resonances in California and Australia: Evidence for intensity modulation by the local height of the D region, *J. Geophys. Res.*, **96**, 15,973, 1991.
- Sentman, D. D., E. M. Wescott, D. L. Osborne, D. L. Hampton, and M. J. Heavner, Preliminary results from the SPRITES '94 campaign: Red sprites, *Geophys. Res. Lett.*, **22**, 1205, 1995.
- Shepherd, T. R., W. D. Rust, and T. C. Marshall, Electric fields and charges near 0°C in stratiform clouds, *Mon. Weather Rev.*, **124**, 920, 1996.
- Stolzenburg, M., T. C. Marshall, W. D. Rust, and B. F. Smull, Horizontal distribution of electrical and meteorological conditions across the stratiform region of a mesoscale convective system, *Mon. Weather Rev.*, **122**, 1777, 1994.
- Stratton, J. A., *Electromagnetic Theory*, McGraw-Hill, New York, 1941.
- Symbalisty, E. M., R. Roussel-Dupré, and V. Yukhimuk, Finite volume solution of the relativistic Boltzmann equation for electron avalanche studies, *IEEE Trans. Plasma Sci.*, **26**, 1575, 1998.
- Taranenko, Y., and R. Roussel-Dupré, High altitude discharges and gamma ray flashes: A manifestation of runaway air breakdown, *Geophys. Res. Lett.*, **23**, 571, 1996.
- Taylor, M. J., and S. Clark, High resolution CCD and video imaging of sprites and elves in the N₂ first positive band emission, *Eos Trans. AGU*, **77**(46), Fall Meet. Suppl., F60, 1996.
- Taylor, M. J., and W. R. Pendelton, CEDAR mesospheric temperature mapper for investigating short period gravity waves, *CEDAR Post*, **29**, 31–32, 1996.
- Wait, J. R., On the theory of the slow-tail portion of atmospheric waveforms, *J. Geophys. Res.*, **65**, 1939, 1960.
- Wait, J. R., *Electromagnetic Waves in Stratified Media*, IEEE Press, Piscataway, N.J., 1996.
- Watanabe, Y., A study on space-time structures of sprites based on photometric observations, M.S. thesis, Dept. of Geophys., Tohoku Univ., Sendai, Japan, 1999.
- Whipple, F. L., Density, pressure and temperature data above 30 km, in *The Solar System*, pp. 491–513, Univ. of Chicago Press, Chicago, Ill., 1954.
- Williams, E. R., Comment on "Thunderstorm electrification laboratory experiments and charging mechanisms" by C. P. R. Saunders, *J. Geophys. Res.*, **100**, 1503, 1995.
- Williams, E. R., The positive charge reservoir for sprite-producing lightning, *J. Atmos. Terr. Phys.*, **60**, 689, 1998.
- Williams, E. R., C. M. Cooke, and K. A. Wright, Electrical discharge propagation in and around space charge clouds, *J. Geophys. Res.*, **90**, 6059, 1985.
- Wilson, C. T. R., On some determinations of the sign and magnitude of electric discharges in lightning flashes, *Proc. R. Soc., Ser. A*, **92**, 555, 1916.
- Wilson, C. T. R., The electric field of a thundercloud and some of its effects, *Proc. Phys. Soc. London*, **37**, 32D, 1925.
- Wilson, C. T. R., A theory of thundercloud electricity, *Proc. R. Soc., Ser. A*, **236**, 297, 1956.
- Yamamoto, M., and T. Ogawa, Source location of ELF Q-bursts, paper presented at 10th International Conference on Atmospheric Electricity, Osaka, Japan, 1996.
- Zipsper, E. J., Use of a conceptual model of the life cycle of mesoscale convective systems to improve very-short-range forecasting, in *Nowcasting*, edited by K. Browning, pp. 191–204, Academic, San Diego, Calif., 1982.

R. Boldi, MIT Lincoln Laboratory, Lexington, MA 02173. (bobb@ll.mit.edu)

S. Heckman, NASA Marshall Space Flight Center, Huntsville, AL 35812. (stan@stanheckman.com)

E. Huang, Massachusetts Institute of Technology, Cambridge, MA 02139. (everest@mit.edu)

W. Lyons and T. Nelson, FMA Research Inc., Ft. Collins, CO 80524. (walyons@frie.com; tnelson@frie.com)

M. J. Taylor, Space Dynamics Laboratory, Utah State University, Logan, UT 84321. (mtaylor@cc.usu.edu)

E. Williams, MIT Parsons Laboratory, Cambridge, MA 02139. (earlew@ll.mit.edu)

C. Wong, J. P. Morgan Securities Asia Pte. Ltd., Singapore 068809. (wong-charles@jpmorgan.com)

(Received August 16, 1998; revised February 17, 1999; accepted February 25, 1999.)